International Journal of Disaster Risk Reduction 142 (2026) 106225

Contents lists available at ScienceDirect

International Journal of Disaster Risk Reduction

journal homepage: www.elsevier.com/locate/ijdrr

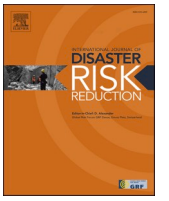

Safeguarding urban functionality: A pre-disaster planning framework for identifying important urban assets in multi-risk recovery

Soheil Mohammadi [a,*], Silvia De Angeli [a,b,c], Nazli Yonca Aydin [d], Giorgio Boni [a], Serena Cattari [a], Francesca Pirlone [a], Tina Comes [e,f]

[a] University of Genoa, Department of Civil, Chemical and Environmental Engineering, Via Montallegro 1, 16145, Genoa, Italy
[b] Université de Lorraine, CNRS, LIEC, F-54000, Nancy, France
[c] Université de Lorraine, LOTERR, F-57000, Metz, France
[d] Technology, Policy and Management Faculty, Department of Multi-Actor Systems, TU Delft, Building 31, Jaffalaan 5, 2628BX, the Netherlands
[e] Faculty Technology, Policy & Management, TU Delft, the Netherlands
[f] Institute for the Protection of Terrestrial Infrastructures, DLR, Germany

ARTICLE INFO

Keywords:
Disaster recovery planning
Multi-hazard risk
Minimum urban system
Betweenness centrality
Temporary shelters
Accessibility equity

ABSTRACT

For recovery to be effective and efficient, proactive measures such as strengthening the resilience of important urban assets must be implemented before disaster strikes. However, existing approaches fail to account for potential consecutive disaster impacts, the transformational changes that happen as a result of the disaster, and the shifting role of urban assets in post-disaster environments. This study presents a methodological framework to support pre-disaster recovery planning in urban areas exposed to multi-hazard risks, namely earthquakes followed by floods. In this study, we develop a methodological framework using a graph-based analytical approach to assess the importance of buildings, roads, census blocks, and temporary shelter areas in urban areas. This method focuses on capturing how the importance of urban assets shifts after consecutive disaster events. Applied to Sanremo, Italy, the methodological framework reveals the vulnerabilities associated with centralized urban planning and a notable mismatch between residential density and the distribution of important assets. The findings underscore how network disruptions and consecutive disasters impact urban connectivity, highlighting the urgent need for decentralized planning and adaptable disaster risk reduction strategies.

1. Introduction

Recovery from disasters involves restoring or improving the economic, infrastructural, social, cultural, and environmental assets, systems, and activities in disaster-affected communities. Increasingly, disaster recovery aims to align rapid restoration with principles of sustainable development and 'Build Back Better' [1].

For an effective and resilient recovery, post-disaster needs and priorities must be placed at the center of planning [2]. Strengthening

* Corresponding author.
E-mail addresses: soheil.mohammadi@edu.unige.it (S. Mohammadi), silvia.de-angeli@univ-lorraine.fr (S. De Angeli), N.Y.Aydin@tudelft.nl (N.Y. Aydin), giorgio.boni@unige.it (G. Boni), serena.cattari@unige.it (S. Cattari), francesca.pirlone@unige.it (F. Pirlone), tina.comes@dlr.de (T. Comes).

https://doi.org/10.1016/j.ijdrr.2026.106225
Received 17 December 2025; Received in revised form 23 May 2026; Accepted 24 May 2026
Available online 26 May 2026

system functionality before a disaster can reduce potential losses and prevent critical functionality decline, making recovery easier [3,4]. However, these needs vary widely depending on the social and geographic context of each disaster-affected area, making it essential to adopt an inclusive, context-sensitive approach [2,5]. Key to taking such a proactive approach is thus identifying and -prioritizing essential infrastructure prior to a disaster, especially when resources are limited [6–8].

In disaster planning, facilities like hospitals, fire stations, and public administration buildings are usually prioritized first, as they are essential for the immediate response [6,9–11]. However, once these are secured, recovery also depends on a wider set of urban functions that keep the community alive and able to rebuild [12–14]. This idea is captured in the "*Safeguarding Limit Condition*" (SLC), which focuses on protecting services, buildings, and spaces that are vital for a city's economy, culture, and social identity. Preserving these elements ensures that recovery can begin promptly and that the continued habitability of the city is safeguarded [15]. As such, addressing the SLC requires a multidisciplinary approach, combining engineering, urban planning, economics, and social sciences. For example, the EQ-DIRECTION method identifies and prioritizes buildings that should remain operational during reconstruction after an earthquake, considering both their structural resilience and their broader value to the community [16].

When shifting from single to multi-hazard recovery planning, the complexity of disaster recovery increases due to the interactions between risk components including hazards, vulnerabilities, exposure, and cascading impacts [17]. While multi-risk approaches attempt to address these challenges, they often fail to fully capture the intricacies of recovery planning [18,19]. Recovery is particularly challenging for consecutive disasters, as one event strikes before the recovery from a previous disaster is complete. Real-world examples illustrating these challenges are the 2017 Iran–Iraq earthquake [2] and the 2023 Türkiye-Syria earthquake [20], where floods after earthquakes disrupted recovery efforts, affected temporary shelter areas, and claimed more lives [21,22].

Current approaches to multi-risk recovery planning only partially capture the complexity of the process. Key limitations include:

- Hazard-centric focus: Existing frameworks focus on the hazards component of the risks [23,24] usually addressing the initial impact of a single, isolated event. This approach often overlooks the dynamic changes in vulnerability following the first disaster [25]. Crucially, the initial disaster often depletes resources, damages critical infrastructure (like health systems or housing), and strains local capacities, thereby increasing the population's and city's vulnerability and creating new pathways for the subsequent hazard to cause greater, non-linear impacts. Furthermore, these models fail to adequately account for the cascading and compounding effects of consecutive disasters [26].
- Lack of integration between Disaster Risk Management (DRM) measures: many approaches fail to consider potential conflicts (asynergies) [27] between DRM measures.

Recent advancements have begun to bridge the gap in multi-hazard modeling by introducing frameworks that account for damage accumulation and incomplete repair between consecutive events. For instance [28], proposed a discrete-time, discrete-state Markovian framework for multi-hazard life-cycle consequence (LCCon) analysis. Their approach effectively models the dynamic performance decay and recovery of deteriorating engineering systems, such as buildings and bridges, subjected to earthquake and flood events alongside gradual environment-induced corrosion. While Otárola et al. focus on the probabilistic estimation of long-term economic and societal consequences (e.g., repair costs and welfare loss) at the asset level, our study builds upon this foundation by shifting the focus toward spatial network interdependencies and recovery planning logistics at the urban scale [28]. Specifically, we investigate how these consecutive disasters transform the *'Safeguarding Limit Condition'* of the Minimum Urban System, focusing on the accessibility of temporary shelters rather than asset-specific repair costs.

This research addresses these gaps by providing a methodological framework to support multi-hazard disaster recovery planning in urban areas. The framework identifies and prioritizes urban assets critical to post-disaster recovery, particularly those necessary for SLC, by evaluating their performance under multi-hazard risk scenarios. The study focuses on earthquakes and floods as a prototypical multi-hazard context, with earthquakes assumed to be the initial event, followed by floods occurring during the earthquake's early and mid-term recovery phase. Some buildings that require major repairs, but not full demolition and reconstruction, remain uninhabitable throughout the early to mid-term recovery phase, as access is restricted or unsafe until substantial repair work is completed. Although these buildings may eventually be restored and reoccupied in the long term, such repairs typically take many months and fall outside the timeframe considered in this study. Consequently, these structures contribute zero habitability during the early and mid-term recovery phase, until repairs are completed and the buildings are officially cleared for safe use [29,30].

Using a graph-based approach, the methodological framework identifies a *minimum urban system* that must be preserved to meet safeguarding limits and ensure effective recovery. The components of minimum urban system include key assets, census blocks, and temporary shelter areas essential for post-earthquake recovery and flood mitigation.

The methodological framework is applied to Sanremo, a coastal city in northwestern Italy, known for its tourism and cultural events, but exposed to seismic events, floods, and landslides [16,31]. Fuzzy Cognitive Mapping (FCM), was used to integrate stakeholder knowledge into pre-disaster recovery planning [15]. Combined with insights from the EQDIRECTION procedure, this approach identified key urban functions essential for recovery, including critical services and socioeconomic assets. While the methodology is applied in Sanremo, it is designed to be generic and adaptable to other urban contexts.

The pre-step for the application of the methodology and the methodology for the identification of the important assets and the assessment of their spatial importance from a multi-hazard disaster recovery perspective are outlined in Section 2. The results of applying this methodology to the Sanremo case study are presented in Section 3 through a series of maps illustrating key findings. Finally, Section 4 discusses the implications of the results, offers recommendations for integrating these insights into policy and practice, and highlights areas for methodological improvement. Conclusions are reported in Section 5.

2. Methodology

As a foundational step, it is important to identify the vital functions that will enable the urban system to begin and carry out the recovery process in efficient and effective way. In this study, a critical services and infrastructures represent *functions* that require a group of assets. For example, education is considered a function, while schools, universities, and other learning institutions are the assets that deliver it. The European Commission [32] identifies 19 distinct societal functions that are essential for recovery. To contextualise the list and integrate community priorities, in our study, vital urban functions are identified through a participatory approach. The process began with the selection of strategic buildings, following the EQ-DIRECTION methodology outlined by Ref. [16]. This was complemented by the use of Fuzzy Cognitive Mapping (FCM), as implemented by Ref. [15], to further identify key

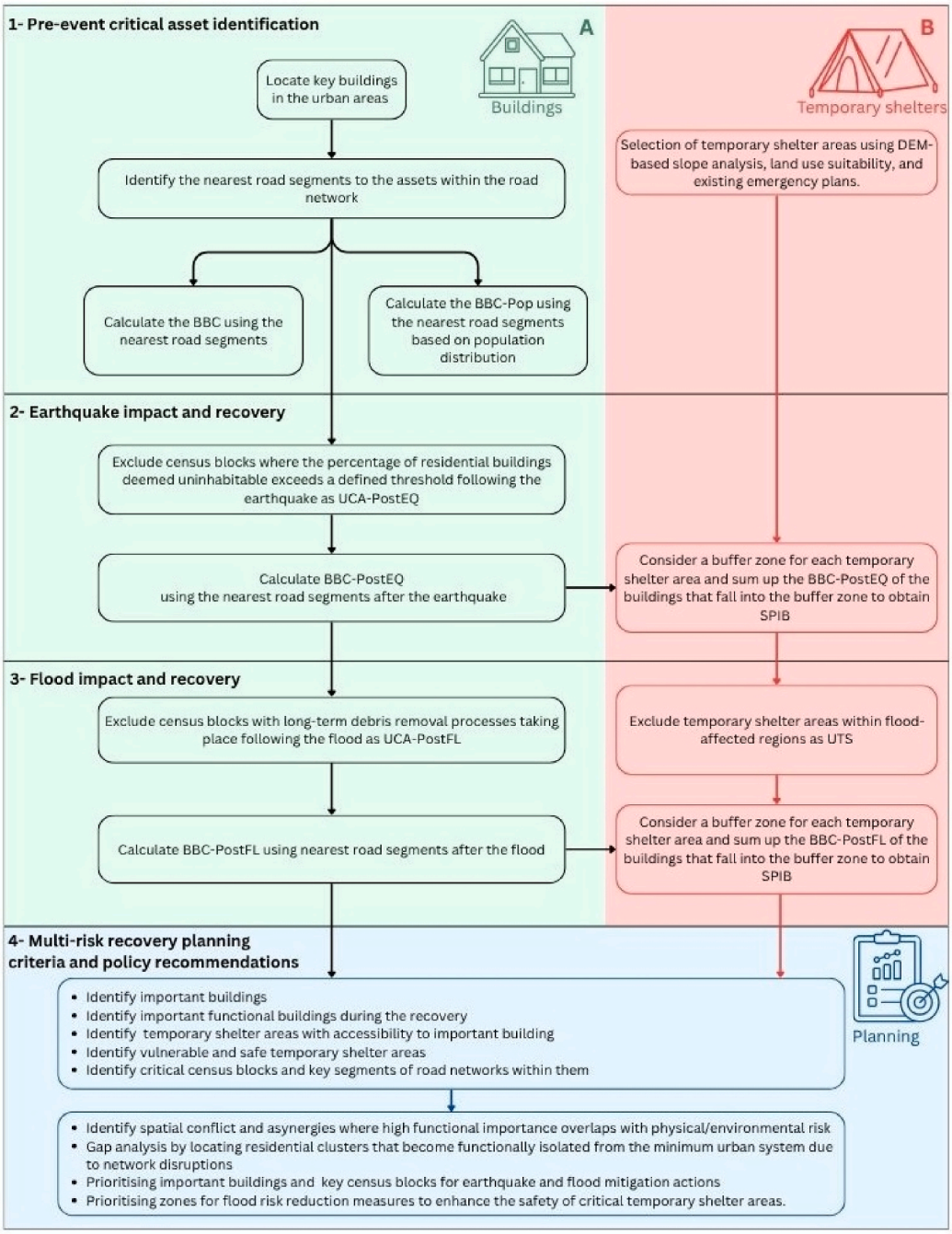

Fig. 1. Overview of the methodology's general workflow.

urban functions by capturing their interdependencies. This identification process serves as a foundational step for applying the methodological framework proposed in this study. Accordingly, the vital urban functions are mapped to the physical assets and built environment considered in the case study (see Section 3.1). These include touristic attractions, essential pharmaceutical services, education facilities, supermarkets and grocery stores, touristic accommodations, and strategic socioeconomic landmarks such as the Casino di Sanremo, the Ariston Theater, and the Mercato Annonario.

Building on the defined scope and identified asset classes, the methodology's workflow (Fig. 1) follows four steps in two parallel tracks for Steps 1 to 3 that are merged into a common synthesis in step for: Track A concerns buildings and assets that are present in the built environment (green in Fig. 1), while Track B focuses on temporary shelters (red in Fig. 1).

In step 1, "Pre-event critical assets identification", for the track A, focusing on buildings the important assets corresponding to vital urban functions and strategic buildings are identified within the urban context. Then considering the transportation network as an intermediary element, graph-based metrics based on Building's Betweenness Centrality (BBC) and Population density-based Building's Betweenness Centrality (BBC-Pop) measure are established to assess the spatial importance of important assets and buildings within the city. Moreover, in the B track, temporary shelter areas' locations are identified using slope analysis, land-use suitability mapping, and a cross-reference with existing municipal emergency plans.

In Steps 2 and 3, we evaluate the impacts of earthquakes and subsequent floods on both the network and the urban area through two parallel analytical tracks (Fig. 1). In Track A we analyze how these disasters affect established BC-based metrics for urban assets, specifically calculating the Post-Earthquake Building Betweenness Centrality (BBC-PostEQ) and the Post-Flood Building Betweenness Centrality (BBC-PostFL). This track assesses the shifting spatial importance of key buildings by excluding census blocks that are rendered uninhabitable or are hindered by long-term debris removal. Simultaneously, in track B we evaluate the temporary shelters locations. We first assess the physical safety of temporary shelters by excluding those located within flood-affected regions as Unsafe Temporary Shelter (UTS). We then measure the functional accessibility of these shelters by calculating the Shelter Proximity to Important Buildings (SPIB). This is achieved by summing the post-disaster centrality metrics (BBC-Post-EQ and BBC-PostFL) of assets located within the buffer zones of each shelter, thereby identifying variations in accessibility to critical services during the recovery phase.

Together, these analyses help us understand the post-disaster recovery condition after the earthquake and after the subsequent flood. In Step 4, the findings from the previous steps are synthesized to establish multi-risk recovery planning criteria and policy recommendations. This phase involves primary identification objectives: identifying important buildings, functional buildings during recovery, and temporary shelter areas based on their accessibility to those buildings. Additionally, it distinguishes between vulnerable and safe temporary shelters and identifies critical census blocks and their associated road network segments. These criteria directly inform the final planning stage, where policy recommendations are formulated to guide mitigation and risk reduction. Specifically, this involves prioritizing important buildings and key census blocks for earthquake and flood mitigation actions. And prioritizing zones for flood risk reduction measures to specifically enhance the safety of critical temporary shelter areas.

2.1. Data collection and processing

The case study area for this analysis covers the entire administrative boundary of the Sanremo Municipality (see section 3.1). The buildings and assets within this area are identified using Google Maps and OpenStreetMap (OSM). In case of differences between these two sources of information, first, the Google Earth images are checked, and if it is not clear, field observations are included to determine the building use. If even one unit in a building has the type of use corresponding to vital functions, the entire building is classified according to that use, regardless of whether other units have different functions or usability. For example, an entire residential building block that contains a single supermarket unit in the ground floor is marked as a supermarket on the map due to the lack of precise information on how much of the building's area is actually designated for the supermarket.

To construct the urban transportation network, OSM data is retrieved using the OSMnx library. First, the road network for the urban area is extracted, considering only drivable roads (network type = 'drive'). This network forms the core representation of vehicular mobility within the city. In addition, a customized pedestrian network is obtained by applying a specific OSM filter (["highway" = "pedestrian"]), ensuring that only pedestrian pathways are included. The resulting pedestrian graph is then combined with the drivable road, allowing both transport modes to be analyzed within a unified framework. Population density values at the census block level are also obtained from the Italian National Institute of Statistics (ISTAT) census data.

To prepare the dataset for post-disaster recovery analysis, additional processing is performed on residential buildings. Building-specific information, including structural material, number of floors, and construction period, is collected from in-situ surveys and the ISTAT census data. These parameters are used in combination with fragility curves to estimate potential structural damage levels for each building (see section 2.3).

Flood hazard information is obtained from the *P.d.B. rilievo regionale – Fasce fluviali* [33](official flood hazard maps approved by the basin authority) dataset available through the Liguria Geoportal, which delineates floodplain zones at the regional scale. Specifically, to evaluate small-scale flash flooding impacts during the post-seismic recovery timeline the official high-probability flood hazard map corresponding to a 50-year return period scenario was extracted. This scenario is explicitly referred as "high probability scenario" by the Italian and Regional regulations. Seismic hazard is characterized using the *Italian Seismic Hazard Map (MPS04)* [34,35], considering a 475-year return period and assuming uniformity across the municipality. Local variations in seismic demand are accounted for by incorporating site amplification effects, estimated from topographic conditions (derived from a Digital Elevation Model – DEMs) and stratigraphic characteristics (based on the Forte geological map [36]).

2.2. Pre-event critical assets identification

2.2.1. Important buildings

To identify critical buildings and assets within the urban environment, the network is considered as an intermediary element to capture spatial importance of buildings and assets within the city. Network centrality measures, introduced by Freeman [37,38], are widely used to identify critical nodes within social, economic, and physical networks. Urban road networks evolve through densification and exploration [39–41], shaping city structure and reflecting functional and social importance, with network-based measures offering a valuable proxy for identifying key areas where infrastructure and population dynamics intersect.

For transportation networks, Betweenness Centrality (BC), which measures how often a node (or edge) appears on the shortest paths between other nodes (or edges), provides a good indicator of critical locations in spatial networks [42]. This metric has been applied in various contexts. [43] used the BC to analyze the role of individual channels in a multi-threaded channel system in Bangladesh, while [40] employed it to study the evolution of road networks in Milan, Italy. Further studies on identifying critical nodes and edges in large-scale physical networks include works by [42,44–46].

In our study, to assess the importance of network edges—and consequently, their location and the buildings linked to these edges—two key measures are employed: Edge Betweenness Centrality (EBC) and Population density-based Edge Betweenness Centrality (EBC-Pop). These metrics allow us to analyze urban space more effectively, identifying areas of critical importance within the city.

EBC is computed using NetworkX, a Python library for creating, analyzing, and visualizing complex networks. In this analysis, edge length is considered as a weight, and EBC quantifies the importance of each edge based on how frequently it appears on the shortest paths within the network [37].

To account for population density, EBC-Pop is introduced as an original contribution, modifying the EBC measure to better reflect the spatial distribution of residents. EBC-Pop is computed to assess the importance of network edges while incorporating population distribution. This process involves modifying the traditional EBC by integrating population density data from nodes into the calculation. First, population density values according to the nodes' location (the census area it is located in) are assigned to the nodes in the network graph. This ensures that each node carries information about its surrounding population density. Population density was selected over absolute population to normalize for variations in census block sizes and to accurately represent 'urban intensity' and user concentration. As density characterizes built-up and urban sprawl [47], it identifies critical areas serving dense residential clusters while preventing large, sparsely populated zones from misrepresenting network demand. Next, a custom function is implemented to compute EBC-Pop, adjusting the standard measure by incorporating population density as below:

$$EBC\_Pop(e) = \sum_{s \neq t} \frac{\sigma_{st}(e)}{\sigma_{st}} \cdot P(s,t) \quad \text{Equation 1}$$

where:

$EBC\_Pop(e)$ is the population density-weighted edge betweenness centrality of edge e.

σ_{st} is the total number of shortest paths between nodes s and t.

$\sigma_{st}(e)$ is the number of those shortest paths that pass through edge e.

$P(s,t)$ is the population density factor associated with the shortest path between nodes s and t, computed as:

$$P(s,t) = \rho_s + \rho_t \quad \text{Equation 2}$$

wwhere:

ρ_s and ρ_t are population density of the census area where nodes s and t are located in respectively.

The EBC-Pop computation process begins by initializing a dictionary to store the betweenness values for all edges. Then, the shortest paths between all pairs of nodes in the graph are determined. For each path, a population density factor is introduced, which accounts for the density values of the source and target nodes. For each shortest path found, the edges forming the path receive an increment in their betweenness score, weighted by the population density factor. This adjustment ensures that edges connecting areas with higher population densities receive a higher importance score compared to those connecting sparsely populated areas. To maintain consistency with standard betweenness centrality, the values are normalized based on the graph's size as below:

$$EBC\_Pop_{norm}(e) = \frac{EBC\_Pop(e)}{(N-1)(N-2)} \quad \text{Equation 3}$$

Where N is the total number of nodes in the network.

To establish the spatial relationship between the identified assets and the transportation network, a geospatial analysis is conducted using GeoPandas, a Python library designed for efficient geospatial data processing and analysis. A nearest-neighbor analysis is performed to determine the closest road segment for each building. A custom function computes the distance between each building point and all road network edges, identifying the nearest edge based on the minimum distance. The corresponding edge ID is then assigned to each building.

Finally, the EBC and EBC-Pop_{norm} of the nearest edges are assigned to their corresponding buildings. As a result, each building is attributed with two key metrics, the Building's Betweenness Centrality (BBC) and the Population density-based Building's Betweenness

Centrality (BBC-Pop), which provide insights into the importance of each building within the urban network.

To provide a clear conceptual foundation for readers unfamiliar with network topology, the fundamental principles and calculation steps of EBC (example 1) and EBC-Pop (example 2) are illustrated through simplified graph examples in Appendices.

2.2.2. Temporary shelters

In step 1, as indicated in Fig. 1 by the track B, to identify suitable locations for temporary shelter areas, a high-resolution Digital Elevation Model (DEM) with a 1-m resolution is utilized. Using the Raster Terrain Analysis - Slope Function in QGIS, the slope of the entire urban area is computed. Areas with a slope below 10° are extracted as potential candidates [48]. A detailed land use assessment is conducted using OpenStreetMap (OSM) tags and Google Earth imagery to identify open, permeable, or paved spaces capable of accommodating large groups. Specific focus is placed on sports facilities (e.g., football fields), public squares, and unbuilt urban plots. Buildings and heavily forested areas are excluded during this stage.

The potential areas identified through the GIS-based filters are cross-referenced with the existing municipal emergency plan. This ensures that the final dataset includes both officially designated sites and newly identified optimal locations, providing a comprehensive pool for subsequent risk assessment.

2.3. Earthquake impact and recovery

In step 2, the impacts of hazards are evaluated on residential buildings to provide a clear understanding of the post-hazard situation and the resulting changes in the positioning and significance of the important buildings during the recovery time and formation of new settings in urban settlements. Note that the impact on important buildings is not included here, as it will need to be evaluated in greater detail separately.

Various methodologies can be employed to assess the impact of earthquakes on residential and urban areas. A crucial aspect of this assessment is determining the probability of exceeding different levels of structural damage and quantifying the expected impact. Given the typically high number of residential buildings within urban settings, the use of simplified vulnerability models is preferable to ensure feasibility in large-scale evaluations.

In this study, the empirical–heuristic vulnerability model [49] is adopted to estimate the damage levels of residential buildings. This model represents an evolution of the macroseismic approach [50] and introduces a significant advancement by incorporating calibration based on observed post-earthquake damage data.

The assessment of seismic impact on the residential building stock is performed using Peak Ground Acceleration (PGA) as the primary intensity measure. While it is recognized that other intensity measures may correlate more efficiently with specific damage states [51–53] in certain contexts, the choice of PGA is consistent with established practice for large-scale seismic risk studies in Italy [54] and aligns with the standard framework for ELC evaluations. Furthermore, since the building stock in the current research case study area is predominantly characterized by low-to mid-rise structures (2 to 4 stories), PGA remains a reasonable and reliable indicator of potential damage within this urban morphology.

The reliability of this approach for the specific context of case study area, is supported by recent comparative studies; for example, in Ref. [55], the heuristic model was compared with a mechanical-analytical approach for the masonry building stock of case study area, demonstrating strong agreement between the two methods.

The seismic input for this framework is characterized using the Italian Seismic Hazard Map (MPS04) and more specifically, values of the intensity measure for a 475-year return period. While it is recognized that a probabilistic hazard map aims to incorporate the influence of different sources of uncertainties (in the case of MPS04 that is pursued by a logic-tree approach to model the epistemic uncertainty in the completeness of the earthquake catalog, the assessment of the seismicity rates and Mmax, and the ground-motion prediction equations) and may not capture the specific spatial correlation of ground shaking inherent in a single, deterministic rupture scenario, the use of a reference hazard map is consistent with the SLC. The primary goal of the SLC and this recovery framework is not to predict the outcome of one specific fault rupture, but to stress-test the 'Minimum Urban System' against a standardized, high-impact design event established by national regulations. To partially account for spatially varying local demands, site amplification effects were incorporated by deriving topographic and stratigraphic factors from a DEM and local geological maps.

Residential buildings' specific parameters such as number of floors, structural material (Reinforced Concrete - RC or Unreinforced Masonry - URM), and age are collected through an in-situ survey and census data are used to compute the vulnerability index (V) for each building. Subsequently, fragility curves are assigned to residential buildings based on three key attributes: height, construction age, and structural material.

Ultimately, the probability of exceeding different damage levels is computed for each census block, considering the collective composition of residential buildings within each block. According to [54] and [56], the percentage of the unsafe residential buildings just after the disaster can be obtained by applying the values reported in Table 1. While some buildings with damage levels 2 and 3 may eventually be repaired and made habitable, as mentioned earlier, our analysis concentrates on the early to mid-term recovery phase,

Table 1
Unsafe building percentages per damage level.

Damage level	1	2	3	4	5
Percentage of unsafe buildings	0	40	100	100	100

when such repairs are not yet completed. Therefore, in the context of this study, "unsafe buildings" refer specifically to those deemed uninhabitable in both the short and long term.

Census areas are classified as Post-Earthquake Unsafe Census Areas (UCA-PostEQ), if more than 15% of the residential buildings within them are deemed unsafe. This threshold of 15% was determined by the research team through an iterative process, balancing the need for granularity in localized risk management with the practical constraints of large-scale post-disaster recovery efforts. It is important to note that this specific value is context-dependent; while the 15% criterion provides a necessary compromise for the demographic and structural characteristics of the Sanremo case study, the threshold should be recalibrated based on local conditions, acceptable risk levels, and spatial granularity (size, population) of the administrative or statistical units used for the analysis, when implementing this methodology in different regions. A lower threshold might lead to an impractical designation of large urban areas as unsafe, whereas a higher threshold could underestimate localized risks, potentially endangering returning residents.

The affected road segments located within the unsafe census area are removed, and Post-Earthquake Edge Betweenness Centrality (EBC-PostEQ) and Post-Earthquake Building Betweenness Centrality (BBC-PostEQ) are calculated for the remaining network and buildings. This adjustment aims to evaluate how the removal of unsafe areas influences the importance of different locations and buildings that play a critical role in the city's recovery during post-earthquake time.

Population weighting is not applied to the post-earthquake betweenness metrics at this stage. Following a major disaster, significant population displacement is expected. However, determining suitable locations to accommodate the displaced population is one of the central objectives of the present research. Therefore, the EBC-PostEQ and BBC-PostEQ values are computed without population weights, focusing instead on the structural and network-based effects of removing unsafe areas.

Census block boundaries usually follow the centerlines of roads (Fig. 2). In our method, certain road segments are removed based on the assumption that the weakest buildings in each census area are those located along the roads. These vulnerable structures, referred to as “interfering buildings” (B1, B2, and B3 in Fig. 2), may collapse and block adjacent streets. To account for this, a 10-m buffer is applied around unsafe census areas (UCA-PostEQs) to exclude the affected road sections (e.g., R1 in Fig. 2). The 10-m distance is chosen because the widest roads in the study area are 20 m, making this buffer a realistic representation of potential blockages.

It is important to note that when a census area is classified as unsafe, we remove only the road network within that area, not the buildings themselves. Residential buildings (B in Fig. 2) are used only as indicators to identify UCA-PostEQs, while important buildings (IM in Fig. 2) remain visible on the map, even if they fall within unsafe areas. This approach gives decision-makers a more comprehensive picture of the post-disaster situation. For example, an important building may still hold significant value assigning new closest edge to it (R3 to IM1 or R2 to IM2) even if it lies inside an unsafe area, in which case alternative access routes might need to be planned.

As shown in step 2 of the track B of the methodology framework in Fig. 1, for addressing earthquake impact and recovery in the area we need to consider a buffer zone around temporary shelter areas to identify buildings within these zones. To align with the concept of pedestrian sheds, which play a crucial role in shaping neighborhoods and communities within urban environments, a 400-m (1/4 mile) buffer is established for each shelter [57,58]. The BBC-PostEQ values of buildings within these buffer zones are then aggregated and assigned to the corresponding temporary shelter areas as shelter proximity to important buildings (SPIB).

2.4. Flood impact and recovery

The relevant difference between earthquake and flood impacts for the procedure presented here lies in the duration of the recovery

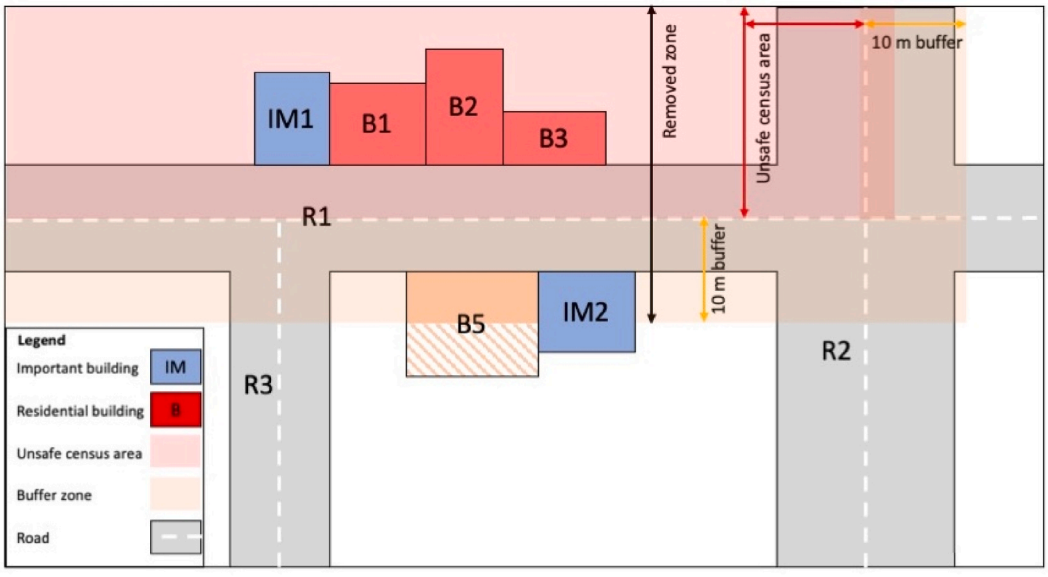

Fig. 2. Schematic representation of unsafe census area removal process and the application of a 10-m buffer to exclude affected road segments.

phase. Flood recovery is generally very rapid [59,60], especially when compared with earthquake recovery [60]. This makes the likelihood that an earthquake occurs during the flood recovery phase negligible, though not impossible.

In contrast, the significantly longer duration of earthquake recovery—which can span several months to years for the early-to-mid-term phases alone—increases the probability of a subsequent flood occurring during this period. This makes the second case far more relevant for the application of the methodology. While the exact duration of these phases is inherently uncertain and depends on specific local socio-economic and administrative factors, the focus of this work is on the early-to-mid-term recovery period, when urban systems are at their most vulnerable and temporary shelters are actively occupied.

Based on these premises, the methodology defines two interaction schemes between earthquake and flood risk, depending on the characteristic scale of the flood phenomenon:

- **For large, highly destructive flood**s occurring during the earthquake recovery phase, interactions may affect each risk dimension (i.e., hazard, exposure, and vulnerability). In terms of hazard, earthquake-induced damage to flood-protection structures can create "additional hazard potential" [61]: the primary hazard (the earthquake) impairs the systems designed to reduce the magnitude of the secondary hazard (the flood). As a result, the characteristics of the subsequent flood, such as its extent and intensity, may change, increasing overall flood risk. At the same time, flood vulnerability may rise due to already damaged buildings, and exposure may increase as displaced populations move into flood-prone areas.
- **For small-scale flash floods**, the magnitude of these events during the earthquake recovery phase is insufficient to trigger additional hazard potential, as they typically occur in areas without major flood-protection structures or with structures too small for earthquake damage to meaningfully affect their performance. Consequently, earthquake impacts do not substantially modify the flash-flood hazard or cause notable changes in vulnerability (flash floods rarely produce structural damage to buildings). The interaction in this case concerns only exposure, particularly in relation to temporary shelters established after the earthquake, where large numbers of people may be concentrated in locations prone to flash flooding, thereby increasing the number of individuals exposed.

The methodological framework is designed to be generic and adaptable to diverse urban contexts and hazard scales. The comprehensive methodological framework details the structural network impacts of large, highly destructive flooding on the built environment (step 3 Track A). Under this scenario, flood induce dynamic performance decay and infrastructural disruptions, initiating long-term debris removal processes within severely inundated urban zones. To operationalize this in the graph-based network, census blocks heavily impacted by post-flood debris accumulation or structural damage that hinders logistical mobility are classified as Unsafe Census Areas Post-Flood (UCA-PostFL). Similar to the earthquake unsafe census area threshold, the specific cutoff criteria utilized to designate a census block as impaired by debris accumulation (UCA-PostFL) is inherently context-dependent and determined through expert judgment. For the flood impact, stakeholders and civil protection experts can calibrate the blockage threshold based on localized factors, such as the ratio of street widths to potential debris volume, or the expected operational constraints of local emergency clearance teams.

Similar to the seismic impact phase, the road network segments falling within these UCA-PostFL zones are removed from the area. The framework then recalculates the network shortest paths to derive the Post-Flood Edge Betweenness Centrality (EBC-PostFL) and assigns these values to the adjacent buildings to determine the Post-Flood Building Betweenness Centrality (BBC-PostFL).

While the track A of Step 3 (Fig. 1) is included to ensure the framework's applicability to large-scale destructive floods—where interactions may affect hazard, exposure, and vulnerability— our case study focuses on the implications of small-scale flash floods occurring during the earthquake recovery phase, and therefore on the red track only. By focusing on the track B of Step 3, the analysis highlights the critical risk of concentrating displaced populations in temporary shelter locations prone to flash flooding, thereby increasing the number of individuals exposed in a post-disaster environment. It is therefore important to ensure that none of these areas can be impacted by floods.

Finally in case of large-scale destructive flood the framework aggregates these updated BBCPostFL values of important buildings falling within the 400-m buffer zones of temporary shelters to compute the post-flood Shelter Proximity to Important Buildings (SPIB), capturing how functional accessibility to critical services fluctuates in the aftermath of a subsequent flood. However, since our case study focuses specifically on small-scale flash floods that do not cause major structural network disruptions, this post-flood SPIB recalculation is omitted from our practical application.

To assess flood impacts, a flood scenario must be defined based on the probability of occurrence of this hazard in the study area. In line with the overall methodology, the scenario is derived from the official flood hazard maps approved by the competent authorities.

According to current regulations (EU Floods Directive), flood hazard mapping must include high-, medium-, and low-probability scenarios. The methodology therefore, adopts the high-probability flood hazard maps as indicators of the areas that have a relevant likelihood of being flooded during the earthquake recovery phase. While the absolute temporal probability of a 50-year event occurring within the early-to-mid-term recovery window (typically estimated in months to years) remains numerically low, its inclusion is justified by the precautionary principle in civil protection planning, ensuring that temporary shelters are not sited in zones officially designated as high-risk. Temporary shelters falling within the inundated areas are classified as *Unsafe Temporary Shelter* (UTS) zones.

2.5. Multi-hazard risk recovery planning criteria and policy recommendations

By following the steps outlined in the methodology, a set of indicators is calculated. Each indicator, either individually or in

combination with others, can correspond to a specific planning criterion, as shown in Table 2. These planning criteria enable stakeholders to make informed decisions on various risk reduction measures and strategically allocate investments.

As the final step of the proposed methodology that is illustrated in Fig. 1, policy recommendations are formulated to guide the implementation of mitigation strategies and risk reduction measures.

To address this step, the indicator maps were examined through a qualitative comparison conducted by the authors. Instead of applying a formal multi-criteria analysis, the evaluation relied on expert judgment to interpret spatial patterns, assess overlaps, and identify discrepancies across indicators. Trade-offs were considered by analysing which areas consistently emerged as critical across several indicators and by noting locations where objectives conflicted—for example, areas important for network connectivity but simultaneously characterized by high exposure. This comparative, expert-based interpretation formed the basis for defining policy recommendations and identifying priority zones for risk reduction. Although the framework can be extended into a structured multi-criteria decision analysis, the intention in this study was to demonstrate the methodological approach through a reasoned, qualitative assessment.

The transition from technical indicators to policy recommendations involves a spatial overlay analysis to identify "criticality hotspots". In this study, the interpretation of these hotspots followed a structured three-step analytical process:

1. Gap analysis: Locating residential clusters that become functionally isolated from the minimum urban system due to consecutive network disruptions (see section 4.3).
2. Conflict identification: Identifying areas where high functional importance (BBC, BBC-Pop, BBC-PostEQ) overlaps with high physical or environmental risk (UCA-PostEQ, UCA-PostFL, UTS) (see section 4.4).
3. Mitigation prioritization: As the final stage of the methodology, policy recommendations are formulated through a qualitative, expert-based interpretation of the spatial patterns and overlaps across all indicators. This prioritization is not applied to the entire urban area; rather, it identifies "criticality hotspots"—specific zones where high functional importance (measured by BBC, BBC-Pop, and BBC-PostEQ) overlaps with high physical or environmental risk (UCA-PostEQ, UCA-PostFL UTS). The interpretation specifically targets asynergies, defined as conflicts between disaster risk management measures. For example, the analysis highlight locations where a temporary shelter is strategically selected for its post-earthquake accessibility but is rendered unsafe by its exposure to flash flooding.

By accounting for the impacts of multi-hazard risks, the recommendations aim to support stakeholders in prioritizing investments for disaster risk reduction in areas where they can safeguard the settlements during the recovery. This targeted approach is intended to enhance the effectiveness and efficiency of post-disaster recovery, ensuring that resources are directed toward interventions that most significantly strengthen urban resilience.

3. Case study application

3.1. Case study description

Sanremo, a coastal town in northwestern Italy on the Mediterranean coast of Liguria, has a population of approximately 52,918 inhabitants, with a slightly higher number of females (27,648) than males (25,270) (Istat, 2021). Beyond its local population, Sanremo is renowned for hosting major sports and cultural events, such as the Milan–Sanremo cycling classic and the Sanremo Music Festival, which annually attracts 41,000 visitors, including guests, organizers, staff, and tourists. This influx of tourists significantly impacts the local economy. Its Mediterranean climate and scenic coastal setting on the Italian Riviera make Sanremo a prominent tourist destination, reinforcing the importance of urban assets and infrastructure in sustaining its economy and identity. Sanremo is vulnerable to a range of significant natural hazards, including seismic events, flash floods, and landslides [16,31]. This diverse exposure to multiple hazards makes Sanremo an ideal case study for investigating disaster recovery and the critical importance of investing in effective recovery strategies in multi-risk conditions.

As explained in Section 2, and drawing on insights from the FCM methodology as well as the EQ-DIRECTION implementation in Sanremo, a set of vital urban functions are identified through two stakeholder involvement processes. From these urban functions, we identify a list of important buildings and assets that are crucial for the delivery of the identified vital functions. In the case study, this list includes touristic attractions (e.g., museums, galleries, monuments), pharmacies, schools, supermarkets and local markets, hotels and motels, and strategic socioeconomic buildings such as the Casino di Sanremo, Ariston Theater, and Mercato Annonario. A detailed

Table 2
Multi-risk recovery planning criteria and the corresponding set of indicators used to determine them.

Planning criteria	Indicators
Important buildings	BBC, BBC-Pop
Functional important buildings during the post-earthquake recovery	BBC-PostEQ
Functional important buildings during the post-flood recovery	BBC-PostFL
Temporary shelter areas close to important buildings	SPIB
Unsafe temporary shelter areas	UTS
Vulnerable census block and key segments of road network within them	UCA-PostEQ, UCA-PostFL, EBC, EBC-PostEQ, EBC-PostFL

description of the stakeholder engagement process is provided in Refs. [15,16].

To provide a clearer insight into population distribution, Fig. 3 presents an overview of both population density and its spatial distribution across the municipality. However, it is essential to recognize that census block divisions vary significantly in size, which directly affects the interpretation of population density. Larger census blocks, often located in less densely built areas, tend to exhibit lower population densities, even though their total population may be substantial. Conversely, smaller census blocks, particularly those near the city center, register much higher population densities due to the smaller size of census areas.

3.2. Results

The methodology described in Section 2 is applied to the case study of Sanremo Municipality, Italy. The results are presented through a series of maps that follow the sequential workflow of the analysis (see Fig. 1). Policy recommendations, which constitute the final step of the framework, are discussed separately in Section 4.

Several of the figures are presented as multi-panel ("combo") layouts to facilitate direct comparison between scenarios or indicators. Each panel, however, is explained in detail within the corresponding subsection to guide the reader through the interpretation. For example, Fig. 6 combines the pre-disaster and post-earthquake betweenness centrality results for both edges and buildings, shown in unweighted and population-density-weighted forms. Likewise, Fig. 8 presents shelter proximity to important buildings across different conditions (pre-disaster, post-earthquake) and flood scenarios exposure. All these components are described systematically in the relevant sections, ensuring a clear and structured understanding of the results.

3.2.1. Pre-event critical assets

The first steps of the methodology involve extracting the road network and identifying buildings associated with vital urban functions. The results of this analysis are shown in Fig. 4. In this study, the reference to building use serves only to illustrate the spatial distribution of facilities with different functions across areas of varying significance.

The network appears to be dense in the central area and to have sparse peripheral connections. The nearest edges, highlighted in black, show primary connectivity paths, connect several facilities across the network, particularly in the central and eastern parts of the study area. As evident from Fig. 4, the density of important buildings is highest in the city center. The inset map provides a zoomed-in view of the urban core, where the location of multiple facility types becomes evident. In this area, supermarkets and hotels are the most frequently represented, while pharmacies and strategic buildings are more sparsely located.

Pharmacies appear less frequent but remain distributed across both the urban core and adjacent areas. Schools, in contrast, are scattered more evenly throughout the territory, including peripheral zones where other services are largely absent. Touristic attractions, though fewer in number, are present in both central and peripheral parts of the network.

Peripheral areas are characterized by sparse and scattered facilities. In these zones, schools and touristic attractions are the most evident, often appearing as isolated points connected by limited nearest edges. Only a small number of supermarkets and pharmacies extend toward the outer network, and hotels are almost absent from the periphery.

Following the methodology, the first step encompasses locating potential and recommended areas for temporary shelters (TS). Fig. 5 presents the TS areas, including those designated by the municipality for sheltering the population in the post-disaster phase, as well as the potential areas identified as suitable for TS. The figure also illustrates the buffer zones of these areas, defined within 400 m away from the edges of the area. Additionally, Fig. 5 depicts the census areas and the distribution of residential buildings across the municipality of Sanremo.

The predetermined TS areas (purple) are mostly concentrated along the southern coastal belt, where the highest density of

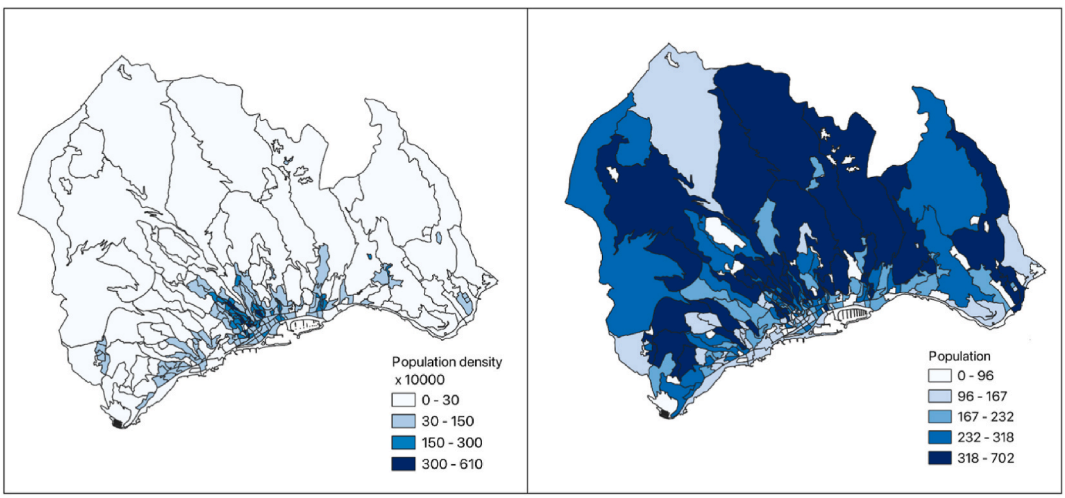

Fig. 3. Population density distribution and absolute population distribution across Sanremo Municipality.

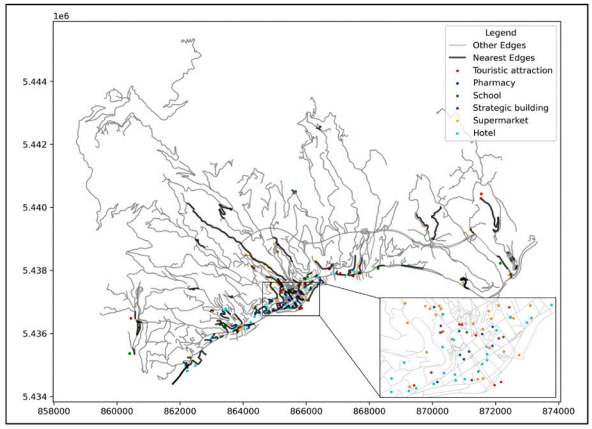

Fig. 4. Extracted road network, important buildings associated with vital urban functions, and their corresponding nearest road network edges determined through a nearest-neighbor analysis.

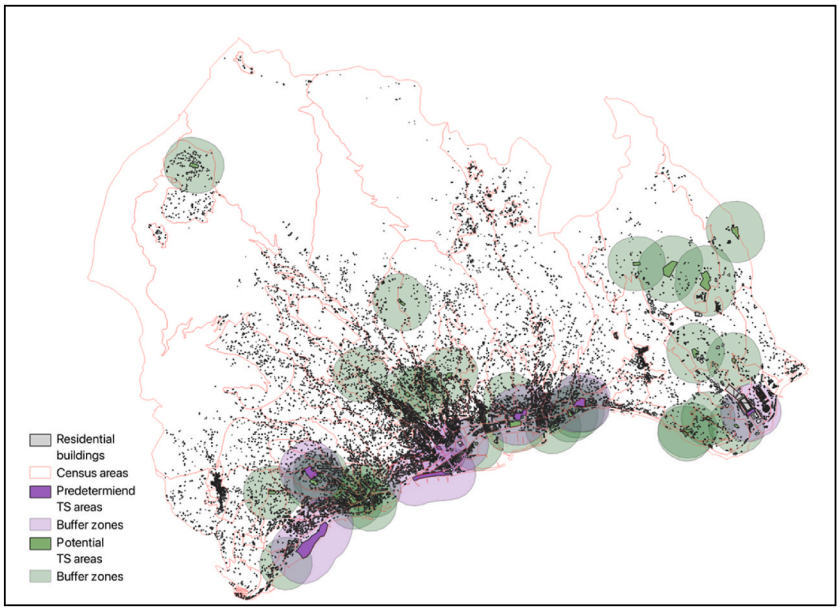

Fig. 5. TS areas, including those officially designated by the municipality for post-disaster sheltering (purple) and additional potential TS areas (green) identified, along with their 400-m buffer zones. The figure also illustrates census areas and the distribution of residential buildings in Sanremo Municipality.

residential buildings is also located. The potential TS areas (green) are more widely scattered across the territory, including both city center and remote inland areas. Several potential TS areas are situated in remote inland zones, with their buffers extending over relatively sparse residential distributions.

In several locations, the buffer zones of predetermined TS areas (purple outlines) intersect with those of potential TS areas (green outlines). However, in some coastal stretches this overlap is limited. In contrast, the dense concentration of overlapping buffers in certain central coastal clusters suggests oversaturation in these zones, while other residential areas remain comparatively underserved. For instance, the eastern and western coastal sections show dense residential clusters with limited or no coverage by either predetermined or potential TS areas.

Fig. 6 (a) and (d), illustrate the EBC and the resulting BBC calculated prior to a disaster. As shown in panel a), the majority of edges with high betweenness centrality are concentrated in the city center, where the density of important buildings is also higher. Additionally, two edges located along the beachfront exhibit notably high EBC values. Consequently, as depicted in 6d, buildings situated near these high-EBC edges have the highest BBC, indicating their strategic position within the urban network. The analysis of building betweenness centrality shows that the majority of nodes have very low values, with most appearing in the lower range of the scale. As expected, some peripheral nodes display near-zero centrality. A concentration of medium-to-high centrality values is observed in the

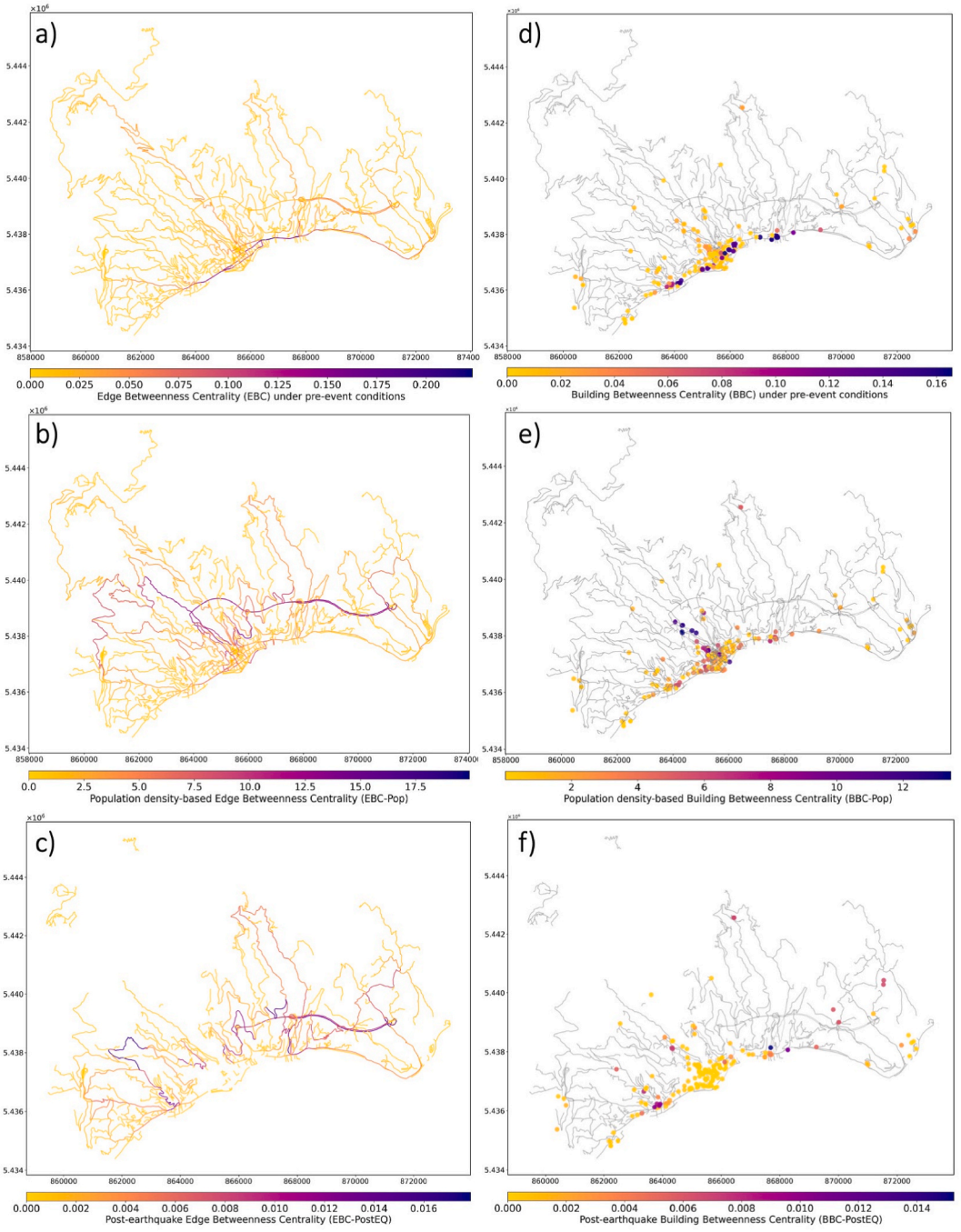

Fig. 6. a) Edge Betweenness Centrality (EBC) under pre-event conditions. b) Population density-based Edge Betweenness Centrality (EBC-Pop) under pre-disaster conditions. c) Post-earthquake Edge Betweenness Centrality (EBC-PostEQ). d) Building Betweenness Centrality (BBC) under pre-event conditions. e) Population density-based Building Betweenness Centrality (BBC-Pop) under pre-disaster conditions. f) Post-earthquake Building Betweenness Centrality (BBC-PostEQ).

central part of the network, particularly in the denser urban core.

In addition to the central cluster, several nodes with relatively high centrality are dispersed across the network. These nodes are not confined to the urban core but are also present in peripheral areas. High-BBC values are not uniformly distributed across dense regions, as some buildings located in the central area show low BBC despite being embedded within the densest parts of the network.The distribution of BBC highlights multiple areas of elevated values rather than a single dominant peak. Furthermore, the nodes with higher BBC appear to align along an east–west corridor within the network, suggesting a linear concentration rather than a purely

radial pattern.

Since the population density reveals an uneven distribution across the municipality, the computation of the EBC-Pop and BBC-Pop produced different spatial patterns compared to the standard EBC and BBC.

As shown in Fig. 6 (b), the most critical edges with high betweenness centrality are no longer concentrated in the city center. Instead, they are distributed across other areas, reflecting the influence of population distribution. Accordingly, Fig. 6 (e) highlights that the most important buildings, based on BBC-Pop, are now located outside the city center, primarily in areas between the city core and residential zones with a high residential population mainly located in northern part of the city according to Fig. 3.

In Fig. 6 (e), buildings with higher centrality values are distributed more widely across the municipality than in the unweighted case. Although high values remain concentrated in the urban core, additional clusters of medium to high centrality emerge outside it, most notably in the northern area, where a distinct group of elevated values appears that is absent in the unweighted results. Overall, Fig. 6 (d) and (e) reveal a clear difference in the spatial extent of high betweenness centrality. The population density–weighted measure produces a broader distribution, with high values occurring in multiple parts of the network, including the northern area. The unweighted measure, on the other hand, shows a more confined pattern, with high values largely restricted to the central and eastern zones. The spatial orientation of high-value buildings also differs. In the weighted figure, the distribution of centrality follows a clearer north–south alignment (Fig. 6 (e)). This contrasts with the unweighted figure, where the distribution of elevated centrality values appears more strongly aligned along an east–west corridor (Fig. 6 (d)).

3.2.2. Earthquake impact and recovery

The assessment of residential building damage under the imposed earthquake scenario (derived from the Italian seismic hazard map for a 475-year return period, see Section 2.2), indicates that a significant portion of the census areas in the city center experience more than 15% of their residential buildings classified as unsafe, both in the short and long term (Fig. 7). Additionally, two large census areas with a high resident population, along with some other scattered census areas, also exhibit a percentage of unsafe buildings exceeding 15%, as shown in Fig. 7.

After removing the areas where more than 15% of residential buildings are classified as unsafe, both in short term and long term, along with the road edges within these areas, the EBC-PostEQ and BBC-PostEQ are recalculated. The results are presented in Fig. 6 (c) and f, respectively.

As shown in Fig. 6 (c), the edges that become important in the road network after the earthquake differ significantly from those that are important during pre-event time. Variations in network connectivity influence EBC-PostEQ by altering the distribution of shortest paths, thereby changing the number of instances in which a given edge is traversed. The resulting network after eliminating the edges due to earthquake impact, is visibly more fragmented, with several connections removed, particularly in the central and northern peripheral areas. In contrast to the denser pre-disaster network, the post-earthquake structure highlights fewer dominant pathways, and the spatial continuity of the network is notably reduced. In the western part of the network, several high-centrality edges extend in a north–south orientation, forming vertical connections between peripheral and more central areas. Toward the eastern portion, additional high-centrality edges are observed, with a mix of east–west and north–south alignments. In contrast, the northernmost and peripheral parts of the network remain almost entirely in yellow, indicating consistently low centrality values.

As a result, as illustrated in Fig. 6 (e), the buildings with the highest BBC-PostEQ values are no longer concentrated in the city center. Instead, several buildings located in more remote areas emerge as important buildings.

The distribution of values shows that the buildings with lowest betweenness centrality scores represented by dark purple dots, account for the majority of the points on the map. These are densely clustered in the central-western area, with additional scattered

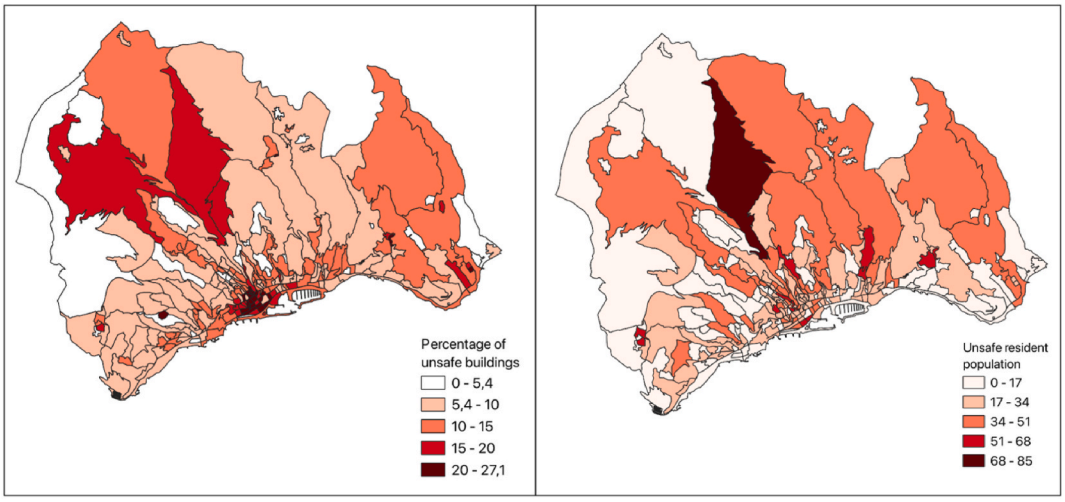

Fig. 7. Percentage of unsafe residential buildings(left) and unsafe resident population (right), both in the short term and the long-term after imposing the earthquake scenario.

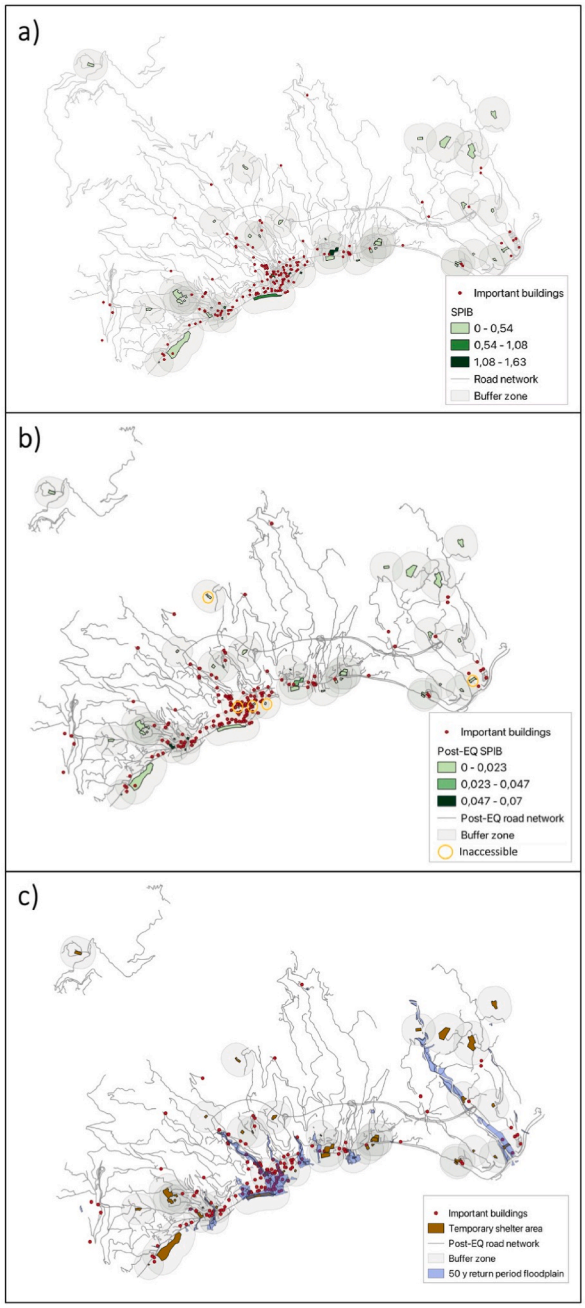

Fig. 8. a) SPIB computed under pre-disaster time, b) SPIB computed under post-earthquake conditions, c) floodplains with 50 years return period and inundated temporary shelter areas.

occurrences extending toward the eastern and northern sections. In contrast, the buildings with highest values, are relatively few and more sparsely distributed. A small number of these higher-value buildings are located near the main concentration in the west, while others appear more isolated along the network toward the eastern part of the map.

As shown in Fig. 8 (a), TS areas are classified into three groups based on the shelter proximity to important buildings (SPIB), which is determined by the presence of important buildings within their buffer zones and their BBC during pre-event time. Notably, TS areas situated in the city center tend to have higher SPIB values.

Fig. 8 (b) illustrates the computed SPIB in the post-earthquake scenario, considering the removal of census areas where more than 15% of residential buildings are deemed unsafe, both in the short and long term. The index in this figure also accounts for the BBC-PostEQ of important buildings. As observed, in this context, temporary shelter areas located in the city center no longer exhibit the highest SPIB values. By removing the edges closest to the temporary shelter areas affected by the earthquake, we identified those

shelters as inaccessible in the post-earthquake environment. As a result, five temporary shelters are classified as inaccessible, three of which are located in the city center as shown in Fig. 8b. A temporary shelter situated in the northern part of the city, though relatively isolated and potentially disconnected from the broader urban network, may still be accessible to the surrounding local population. Given that access within its immediate area remains feasible, this shelter is not classified as inaccessible.

3.2.3. Flood impact and recovery

To address the impacts of a subsequent flood impacting the municipality of Sanremo during the earthquake recovery, the official high-probability hazard maps for a return period of 50 years have been overlaid onto the case study area. As mentioned in Section 2.3, this analysis specifically focuses on the impact of flood on sheltering areas. The overlap of the flood map reveals that some temporary shelter (TS) areas, particularly those located in the city center, fall within unsafe zones. As shown in Fig. 8 (c), three predefined TS areas and three potential TS areas are directly affected by flooding. Among these impacted TS areas, only one retains a high SPIB in the post-disaster scenario. However, when considering pre-disaster SPIB, four of the flood-affected TS areas initially held high SPIB values. These areas are classified as unsafe temporary shelters (UTS).

4. Discussion

Beyond the specific findings from the Sanremo case study, this research proposes a transferable methodological framework for pre-disaster recovery planning in multi-hazard urban contexts. The framework addresses a key limitation in existing disaster risk management approaches by treating urban assets' importance as dynamic rather than static, explicitly accounting for how accessibility, connectivity, and functional priorities shift between pre-disaster and post-disaster conditions.

Another methodological innovation is the integration of population-weighted and unweighted centrality metrics across different temporal stages. The parallel use of EBC/BBC and EBC-Pop/BBC-Pop enables the framework to distinguish between locations that are structurally central within the network and those whose importance is amplified by population concentration. This distinction is critical for identifying unequal access to key assets and services, as areas with high structural connectivity may not correspond to those serving the largest or most vulnerable populations. Such systemic inequalities can exacerbate vulnerability and reduce overall system resilience, particularly when critical services remain accessible primarily to a limited portion of the urban population [62,63].

From a recovery perspective, these inequalities become more pronounced when populations are displaced and accessibility patterns shift. By recalculating centrality measures under post-disaster conditions, the framework tries to reveal how pre-existing disparities may widen, and how areas and population that were previously marginal may become functionally isolated [64].

The framework also addresses the issue of asynergies between disaster risk reduction measures, highlighted in the multi-risk literature. By embedding consecutive hazards within a single analytical workflow, it reveals how decisions that appear optimal under pre-disaster or single-hazard conditions, such as the placement of temporary shelters, may become ineffective or unsafe in the context of consecutive disasters. This shifts planning away from hazard-specific optimization toward planning measures that remain effective under multiple, potentially sequential events [18,19,65].

Finally, the methodology supports an adaptive and modular planning approach. Thresholds, hazard scenarios, and asset typologies can be adjusted to reflect local contexts, data availability, and governance needs. As such, the framework offers a practical tool for supporting pre-disaster decisions that remain effective under post-disaster transformation.

4.1. Identification of the urban core and distribution of critical assets

The spatial concentration of important buildings in Sanremo's historical center reflects a well-established pattern in Mediterranean cities, where administrative and important functions remain anchored in the older urban core [66]. However, when interpreted through a resilience lens, this pattern represents vulnerability for the system. The literature on urban resilience emphasizes the risks associated with concentration of the important function in specific area. When essential services and institutions are geographically clustered, disruptions in the urban core can disproportionately affect the entire system [67,68]. In Sanremo, peripheral neighborhoods with substantial residential density but limited access to important buildings exhibit a form of spatial service dependency, which has been identified as a key determinant of vulnerability in crisis situations [69].

The EBC results further highlight this issue by revealing how movement throughout the municipality is funneled into a limited number of streets. While it is expected that central areas possess high betweenness due to their role in linking different urban sectors, the emergence of two corridors, with high betweenness centrality, extending beyond the historical core is particularly notable. In the urban road network resilience literature, such network chokepoints are recognized as critical elements whose disruption can cause cascading failures, fragmenting mobility and compromising access to services [70,71]. The Sanremo's urban resilience is highly dependent on these corridors and their removal leads to sharp drops in overall network performance and accessibility to essential services.

The BBC analysis reinforces this interpretation by showing that buildings located along these corridors hold disproportionately high functional importance. This aligns with studies that argue for a shift from node-centric to flow-centric understandings of urban resilience, where the resilience of a system depends not only on the characteristics of places but also on the continuity of movement and access between them [72].

In Sanremo, the building–network interdependencies reveal a system where mobility operates through several functional hubs, yet essential services remain concentrated in the historical core. This functional polycentricity combined with service monocentricity creates a structural imbalance that limits redundancy and increases vulnerability. In this sense, if the accessibility to the central service

hub through the emerged corridors is disrupted, multiple peripheral functional hubs lose access simultaneously, reducing the city's resilience during recovery.

4.2. Population density and spatial mismatch in urban functions

The variation in census block sizes can lead to an uneven representation of population density, potentially distorting spatial analyses. For instance, some areas with relatively high total populations may appear underpopulated simply because they cover a vast geographical extent as shown in Fig. 3. Meanwhile, compact urban zones with a smaller surface area may seem disproportionately dense. Therefore, while population density remains a valuable indicator for demographic distribution, it must be interpreted in relation to the spatial characteristics of each census block to avoid misleading conclusions. The size and shape of administrative or census units can strongly affect how population density and urban patterns are represented and interpreted; hence, the spatial scale and configuration need to be carefully considered when analyzing population data.

Despite these variations, the calculation of EBC-Pop and BBC-Pop, as shown in Fig. 6 (b) and (e), reveals a fundamental shift in the urban areas' importance. When population density is incorporated as a weighting factor, the most significant areas of the city shift northward, aligning with the primary residential zones rather than the historical center. Analyzing the EBC-Pop values presented in Fig. 6 (b), it becomes evident that certain edges exhibit high EBC-Pop values despite the absence of important buildings in their vicinity. This finding underscores a critical imbalance: while a large portion of the resident population is located in these northern areas, the concentration of important buildings remains in the city center, resulting in a spatial mismatch between residential zones and key urban functions.

It is crucial to reiterate that this study does not evaluate the usability or operational capacity of these important buildings; rather, they are considered as vital urban elements serving resettled populations for various purposes, including commerce, employment, education, essential services, and socio-cultural identity. As indicated before, the clear spatial separation between major residential areas and important buildings necessitates daily movement between areas with a high number of residential buildings and the central urban core, reinforcing the importance of the road network's segments and their location that connect these two zones. Consequently, the connective corridors linking residential districts to the city center play a crucial role in the urban system. These corridors drive the evolution of the road network, adapting to the increasing demand for accessibility and mobility. As a result, higher EBC-Pop and BBC-Pop values are observed along these pathways, reflecting their growing significance in facilitating movement and connectivity within the city.

A clear distinction can be observed between EBC and EBC-Pop, as well as between BBC and BBC-Pop, by comparing Fig. 6a and b, and Fig. 6 (d) and e, respectively. While both criteria highlight the significance of areas that connect the city center to peripheral neighborhoods, there are notable differences in their spatial emphasis. EBC and BBC place greater importance on the eastern and western parts of the city, whereas EBC-Pop and BBC-Pop emphasize the northern areas. The differences between traditional centrality measures (EBC and BBC) and population-weighted measures (EBC-Pop and BBC-Pop) indicate that the most structurally important roads, as identified by network-based evaluations, do not always coincide with the areas where the highest resident population densities are located. This suggests that road network development and population distribution may have followed different historical, social, or economic factors. For instance, certain neighborhoods might have developed due to economic opportunities, land availability, or historical settlement patterns, and since the city has hilly and mountainous terrain, road construction may have been guided more by feasibility than by ideal connectivity. This can result in a network that prioritizes passable routes expansion rather than the most efficient direct connections. A similar observation was made in Casali et al. (2024) where authors found that average road betweenness centrality showed weak correlation with socioeconomic indicators and followed a distinct evolution pattern illustrating a decoupling between road network development and socioeconomic co-evolution of the urban fabric.

These variations underscore the importance of adopting a multi-faceted approach when analyzing urban connectivity, particularly when using it as a basis for identifying key areas within a city. This is especially crucial in disaster resilience planning, where a comprehensive understanding of both network efficiency and population distribution is essential for effective recovery. Furthermore, there is a need for a shift in urban planning approaches. Traditional urban planning that concentrates key functions within the historical core may no longer be adequate in addressing the complex and evolving realities of modern cities under disaster context. Urban planning should be embedding temporal dynamics and resilience thinking into spatial decisions [73].

4.3. Impact of the seismic events on urban connectivity and gap analysis

The results of the simulated earthquake scenario reveal a high physical vulnerability of the historical city center. Additionally, given the significant population density in the affected census areas, and two highly populated census areas in the northern part of the city, a considerable number of residents are likely to be displaced. This indicates that the pre-disaster urban structure undergoes substantial transformation following a seismic event, leading to major shifts in accessibility and connectivity within the city.

Fig. 6c illustrates the EBC-PostEQ, which serves as an indicator of the importance of various urban areas. The removal of central areas due to earthquake-induced damage results in a decrease in the importance of areas that play the role of a corridor between the city center and the surrounding neighborhoods. As seen in Fig. 6c, this disruption effectively divides the city into two main sections, along with several isolated pockets. Notably, the northern parts of the city, now disconnected from the central core, may face additional challenges in accessibility and the residents of these areas need to be relocated unless they can sustain independent socioeconomic activities. Through this gap analysis, the framework locates specific residential clusters that become functionally isolated from the minimum urban system due to the network disruptions.

Although this division is unlikely to persist in the long term, as post-disaster recovery efforts would aim to restore connectivity through measures such as airlifts, temporary bridges, or alternative transport routes, a critical question arises: to what extent can a single restored connection compensate for the multiple lost connections between these separated urban sections in terms of the capacity? Moreover, if the displaced population from the central areas is relocated to temporary shelters, restoring road connections alone may not be sufficient to fully reintegrate the two urban halves.

In addition to the road network, the presence and functioning of important buildings in the historical center during the recovery phase play a crucial role. These buildings, commercial, administrative, retail, and social service facilities, are central to the socio-economic reactivation of the city centre. They help draw people, goods, and activities back to the urban core and act as anchors that re-establish connections between the separated parts of the urban as the result of earthquake impact.

Fig. 6f presents the BBC-PostEQ, highlighting how the importance of buildings shifts in response to network disruptions. As previously indicated by the BBC-Pop as well, certain buildings in the northern section of the city center remain important, even though large census areas to the north have been severely affected or removed. Moreover, some peripheral buildings, far from the historical core, also become newly critical for supporting basic urban functionality.

4.4. Shifting of the importance of temporary shelter areas due to consecutive hazard events and conflict identification

Analyzing the location of TS areas and their SPIB values during both pre-disaster and post-earthquake conditions, as depicted in Fig. 8 (b) and (c), reveals a significant shift in their relative importance. The city center emerges as the suitable location for these areas, given the concentration of important buildings nearby and their initially high SPIB values. This likely influenced municipal stakeholders' decision to designate three out of eight predefined temporary shelter areas within the city center. However, when considering the impact of the earthquake, only one of these predefined TS sites retains a high SPIB, while the others—both inside and outside the city center—experience a substantial decline in their strategic importance.

Notably, certain potential TS sites in the western part of the city maintain relatively high SPIB values both before and after the disaster. However, these areas are not extensive. In contrast, a large predefined TS area in the western part of the municipality appears to have limited SPIB, likely due to its considerable distance from key buildings, the city center, and major urban corridors, reducing its overall effectiveness in post-disaster conditions.

Analyzing flood maps with a 50-year return period reveals that a significant portion of the city center becomes inundated. Therefore, it can be argued that several TS areas located in the city center, which appeared suitable under pre-disaster conditions, may no longer be capable of providing safe and effective services in the post-disaster environment. This indicates that selecting TS areas solely based on their pre-disaster SPIB may lead to critical shortcomings. Considering that transformational changes often occur in post-disaster environments, and that population vulnerabilities may decrease when facing consecutive hazards such as floods, it is crucial that the selection of TS areas does not rely solely on pre-disaster conditions. Otherwise, the selected areas based on the pre-disaster situation possibly become less strategically located relative to important buildings in the aftermath of a disaster, and also becoming unsafe (i.e., rendered as UTS) in the event of flooding, further undermining their effectiveness as TS areas.

This conflict identification provides a concrete example of the lack of integration between disaster risk management measures and the resulting asynergies discussed by [27,74]. Pre-determined TS areas in Sanremo were largely designated based on pre-disaster conditions and proximity to important buildings, resulting in high SPIB values under normal circumstances. However, when earthquake-induced network disruptions and flood hazards are considered together, several of these same areas lose their strategic importance or become unsafe. Measures that appear effective when evaluated in isolation, such as centrally located shelters optimized for accessibility, can therefore conflict with other risk dimensions, such as flood exposure. This highlights how DRM decisions that do not account for multi-hazard interactions and post-disaster transformations may inadvertently reduce system resilience rather than enhance it.

The multi-hazard context of this study highlights that effective recovery in a multi-risk environment cannot be achieved by simply combining individual hazard recovery and resilience measures. The findings in Sanremo show that network corridors which are structurally robust for seismic recovery may be the most vulnerable to subsequent flash floods. Consequently, policy recommendations must move beyond single-hazard safety; for instance, relocating a temporary shelter is not simply about finding a flood-safe plot, but about ensuring that the new location maintains its 'Post-Earthquake SPIB' so that displaced populations retain access to the minimum urban system throughout the extended recovery duration.

4.5. Integration of stakeholder inputs in the methodological workflow

The framework is designed for decision-makers to tailor the outputs to local strategic needs. The modular structure ensures that core elements can easily be adapted to different contexts as follows:

Firstly, stakeholders determine which functions and corresponding assets are included in the minimum urban system. In Sanremo, this was achieved through FCM to capture local interdependencies and priorities.

Second, decision-makers can adjust the risk tolerance levels. The UCA-PostEQ classification currently uses a 15% damage threshold. Stakeholders can adjust this percentage based on local risk tolerance or the specific capacity of their emergency response teams; a lower threshold prioritizes a more cautious recovery, while a higher one focuses on only the most severely impacted zones. Similarly, the choice of the initial hazard intensity (e.g., a 475-year return period earthquake) and the subsequent flood probability (e.g., a 50-year return period map) is a policy decision. Stakeholders can test worst-case versus most-likely scenarios to see how asset importance shifts under different disaster magnitudes.

Table 3
Summary of methodological assumptions and transferability limits.

Category	Key Assumption	Rationale	Applicability & Transferability Limits
Network Dynamics	Shortest path navigation (Betweenness Centrality)	Represents the most efficient movement for emergency and recovery logistics.	Assumes users have perfect information; Model performance is sensitive to physical disruptions (debris, blocked access) that vary in chaotic post-disaster states
Social Demand	Population density as a weight for EBC-Pop/BBC-Pop	Aligns structural importance with the spatial distribution of residents.	Relies on baseline deviations; may not account for fluid, real-time population displacement.
Systemic Failure	15% damage threshold for road exclusion	Represents a critical mass of interfering buildings likely to block road segments.	Must be recalibrated based on building-to-road width ratios and local construction quality.
Multi-Hazard Timing	Flood occurs during early/mid-term seismic recovery	Previous experiences of consecutive events during the lengthy seismic reconstruction phase.	Specific to regions with overlapping seismic and hydro-meteorological hazard profiles.

Third, regarding the prioritization of road segments, while the current EBC-Pop and BBC-Pop metrics utilize population density, stakeholders can introduce different weighting factors, such as social vulnerability indices or economic output per block, to shift the importance of road segments toward underserved or high-value districts.

By adjusting these parameters, the framework moves from a purely mathematical model to a context-sensitive decision support system that reflects the specific recovery objectives of the municipality.

4.6. Advancement network-based recovery planning approaches

This research advances traditional network-based recovery planning approaches by shifting the analytical focus from static, single-hazard snapshots to an evolving, multi-hazard process. We do so, by (a) shifting the focus on metrics that integrate the social dynamics, and (b) by explicitly planning for disaster sequences.

While network-based approaches often use Betweenness Centrality to identify structural bottlenecks in a given environment, our framework introduces population density-based betweenness centrality as a way to align network importance with actual social demand. By using this measure across consecutive earthquake and flood scenarios, our approach captures the transformational shifts that occur when consecutive disasters alter the urban system before recovery from the initial event is complete.

By explicitly considering two consecutive events, unlike approaches that analyze urban assets in isolation, our approach explicitly considers cascading effects and interdependencies, highlighting how recovery solutions for one hazard, such as centrally located temporary shelters, may become vulnerable under a subsequent hazard, such as flooding. Consequently, this approach provides a more systemic and adaptive tool for pre-disaster planning than traditional single-hazard approaches, ensuring that prioritized assets remain functional through the complex, evolving stages of multi-risk recovery. Our approach also flexible to integrate different types of compounding or consecutive hazards that may be relevant in other contexts and settings.

5. Conclusion

This research presents a methodological framework aimed at enhancing multi-hazard risk recovery planning in urban environments. By focusing on the prioritization of urban assets that are important for post-disaster recovery, particularly those essential for safeguarding the settlement and continuity of urban life during the recovery, the study contributes a structured approach to pre-disaster recovery planning. The framework accounts for consecutive hazards, specifically earthquakes followed by floods, reflecting real-world disaster patterns.

Applied to the case of Sanremo, Italy, the study reveals a concentration of important assets in the historical city center but also a significant spatial mismatch between high-density residential areas and essential urban functions. This disconnect highlights the need for improved connectivity, more balanced urban development, and decentralized planning strategies.

Through advanced network-based metrics such as EBC, BBC, and their population-weighted counterparts (EBC-Pop and BBC-Pop), the study demonstrates how urban connectivity and asset importance shift under both pre-event time and disaster conditions. Moreover, the impact of consecutive hazards, particularly the flooding of temporary shelter areas after an earthquake, emphasizes the necessity of integrated, multi-risk perspectives in planning.

Apart from that, several key takeaways emerge from the research. First, decentralization should be a fundamental consideration for stakeholders and decision-makers. The concentration of critical socio-economic activities, particularly in the city center, can reduce the overall resilience of the urban system. Any disruption in such concentrated areas may severely impair the recovery process, highlighting the need for a more spatially balanced urban development strategy.

6. Limitations, sensitivity, and transferability of the framework

The significance of the findings in this study lies in their ability to provide stakeholders with a framework for identifying priority areas for improvement and investment. However, selecting the optimal intervention areas requires further analysis, ideally through structured decision-making methodologies that incorporate economic and financial cost of the disaster risk reduction interventions [74].

Additionally, improving data collection and availability, particularly concerning socio-economic aspects, is essential for informed planning. The current delineation of census areas does not adequately capture the complexity of urban dynamics. There is a need for more categorized, accessible, and reliable data on economic activities across different urban areas and in various scales.

6.1. Uncertainty in input data and impact on result interpretation

The methodological framework presented in this study relies on several deterministic inputs, which introduces inherent uncertainties that must be considered when interpreting the spatial priority maps. While the results provide a clear roadmap for identifying critical urban assets, the following areas of uncertainty are of particular note:

- Population distribution and dynamics: The population density used in the population density based metrics is based on static census data, expressing where people live. Disasters trigger rapid andpopulation displacement that are also represented by the shelter locations. If a significant portion of the population moves to temporary shelters or leaves the municipality entirely, the demand-side importance of certain road segments may shift away from the residential northern areas and back toward the surviving functional

corridors. As such, the population-weighted metrics serve to measure a transformative shift from the baseline rather than keeping dynamically track of where people are presently based.

- Flood exposure scenarios: The flood analysis utilizes official 50-year return period hazard maps to identify UTS zones. These maps are deterministic and may not account for the altered hydrologic conditions or blocked drainage systems common in post-earthquake environments, which could expand the actual inundated areas beyond the predicted boundaries. In addition, climate change may shift the likelihood of flooding, leading to higher actual return periods than planned for.
- Threshold sensitivities: The classification of UCA-PostEQ in this study is based on a 15% damage threshold. As noted, this value represents a consensus of the research team opinion for the case study. Therefore, the threshold should be recalibrated based on local conditions, acceptable risk levels, and spatial granularity (size, population) of the administrative or statistical units used for the analysis. A minor increase or decrease in this threshold could significantly alter the fragmented state of the post-disaster road network and, consequently, the resulting betweenness scores.

By acknowledging these uncertainties, we would like to highlight the positioning of our approach as strategic decision-support. Decision-makers can and should interpret these findings as an identification of critically hotspots that are likely to be critical across a range of probable scenarios, rather than as exact predictions of point-specific failure. Future work could incorporate probabilistic modeling or sensitivity analyses to quantify how these uncertainties propagate through the multi-hazard recovery workflow.

6.2. *Methodological assumptions and transferability of the framework*

The robustness of the proposed framework lies in its modular structure, allowing for the recalibration of key parameters to fit different urban morphologies and hazard intensities. To ensure transparency and support the transferability of this approach to other urban contexts, Table 3 summarizes the core assumptions and their limiting factors.

CRediT authorship contribution statement

Soheil Mohammadi: Writing – review & editing, Writing – original draft, Visualization, Methodology, Formal analysis, Conceptualization. **Silvia De Angeli:** Writing – review & editing, Visualization, Supervision, Conceptualization. **Nazli Yonca Aydin:** Writing – review & editing, Supervision, Conceptualization. **Giorgio Boni:** Writing – review & editing, Supervision, Conceptualization. **Serena Cattari:** Writing – review & editing, Supervision, Conceptualization. **Francesca Pirlone:** Writing – review & editing, Supervision, Conceptualization. **Tina Comes:** Writing – review & editing, Supervision, Conceptualization.

Declaration of competing interest

The authors declare that they have no known competing financial interests or personal relationships that could have appeared to influence the work reported in this paper.

Appendices

Table a
Overview of the datasets used in this research, including their sources and key information.

Dataset/Source	URL	Data year/Version	Granularity	Notes
OpenStreetMap (OSM)	https://www.openstreetmap.org/	January 2025	Street-level vector data (nodes, edges, attributes), Building footprint polygons and POI tags	Includes roads, intersections, geometry, and metadata. Extracted using network_type = 'drive' and 'pedestrian'. Used to identify building footprints and associated functions. Checked against Google sources for conflicts.
OSMnx Library (data interface to OSM)	https://github.com/gboeing/osmnx	OSMnx v1.9.3	Converts OSM data into a directed graph model	
Google Maps	https://maps.google.com/	January 2025	Building-level and parcel-level POI data	Used to identify building functions (schools, supermarkets, hospitals, etc.). Labels used when available.
Google Earth	https://earth.google.com/	Imagery dates vary by tile; checked at time of analysis (2024–2025 imagery)	High-resolution satellite imagery	Used when Google Maps and OSM disagreed on building use.
ISTAT Census Data (Buildings & Population)	https://www.istat.it/	2021 Permanent Census (latest complete release	Census block (sezione di censimento) for population; building-	Provides building characteristics (material, floors, construction period) and population density. Used

(*continued on next page*)

Table a (*continued*)

Dataset/Source	URL	Data year/Version	Granularity	Notes
		available during analysis)	level attributes for structural data	to assign structural parameters to each building and population distribution across the census blocks
P.d.B. Rilievo Regionale – Fasce Fluviali (Flood Hazard Zones)	https://geoportale.regione.liguria.it	Latest available regional release at time of analysis (2023–2024 update)	Regional scale; floodplain zoning polygons	Used to identify flood hazard extent for consecutive-hazard analysis.
Italian Seismic Hazard Map (MPS04)	https://ingv.it	MPS04 official release (2006), still the national reference	National grid (0.05°); municipality-level PGA extracted	Used assuming 475-year return period; uniform seismic hazard applied across Sanremo municipality
Digital Elevation Model (DEM)	https://tinitaly.pi.ingv.it/	TINITALY/1.1. (2023)	10 m	Used to estimate topographic amplification factors by deriving slope and terrain classification.
High-Resolution Digital Elevation Model (DEM – 1 m)	https://geoportal.regione.liguria.it/	Latest available regional DEM (e.g., 1-m LiDAR-derived DEM, 2023	1 m	Used to compute slope across the urban area; areas with slope $<10^{\circ}$ extracted for temporary shelter suitability.
Municipal Emergency Plan (Piano di Emergenza Comunale)	Comune di Sanremo, Studi di Microzonazione Sismica di Livello 3 e Definizione della Struttura Limite Urbana (SUM). Università degli Studi di Genova – DICCA.	2021	Location-level designated areas	Official list of pre-designated temporary shelter sites included in the municipal emergency planning documents.

Table b
Abbreviations and their definitions

Abbreviations	Definition
BBC	Building's Betweenness Centrality
BC	Betweenness Centrality,
DEM	Digital Elevation Model,
DRM	Disaster Risk Management
EBC	Edge Betweenness Centrality
FCM	Fuzzy Cognitive Mapping
ISTAT	Italian National Institute of Statistics
OSM	OpenStreetMap
BBC-Pop	Population density-based Building's Betweenness Centrality
BBC-PostEQ	Post-Earthquake Building Betweenness Centrality
BBC-PostFL	Post-Flood Building Betweenness Centrality
EBC-Pop	Population density-based Edge Betweenness Centrality
EBC-PostEQ	Post-Earthquake Edge Betweenness Centrality
EBC-PostFL	Post-Flood Edge Betweenness Centrality
PGA	Peak Ground Acceleration
POI	Point of Interest
RC	Reinforced Concrete
SLC	Safeguarding Limit Condition
SPIB	Shelter Proximity to Important Buildings
TS	Temporary Shelter
UCA-PostEQ	Post-Earthquake Unsafe Census Areas
UCA-PostFL	Post-Flood Unsafe Census Areas
URM	Unreinforced Masonry
UTS	Unsafe Temporary Shelter

Example 1.

Step 1

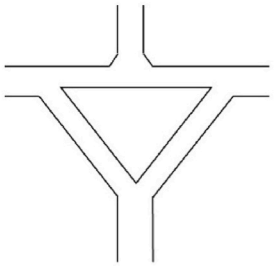

Step 2

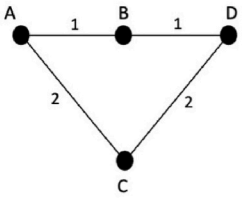

Step 3

Source	Target	Shortest Path(s)	Total Length	# Paths
A	B	A–B	1	1
A	C	A–C	2	1
A	D	A–B–D	2	1
B	C	B–A–C ; B–D–C	3	2
B	D	B–D	1	1
C	D	C–D	2	1

Step 4

Edge	Contributions
A–B	1 (A→D) + 0.5 (B→C) = 1.5
B–D	1 (A→D) + 0.5 (B→C) + 1 (B→D) = 2.5
A–C	1 (A→C) + 0.5 (B→C) = 1.5
C–D	1 (C→D) + 0.5 (B→C) = 1.5

This diagram illustrates the four-stage process of calculating Edge Betweenness Centrality (EBC) for a simplified road network. Here is the step-by-step description:

Step 1 Real-World Geometry

The process begins with a physical road layout.

Step 2 Graph Abstraction and Weighting

The physical map is converted into a Mathematical Graph. Nodes (A, B, C, D): These represent key intersections. Edges: These represent the road segments connecting the nodes. Weights (1, 2): Each edge is assigned a "cost" based on its physical length. For example, the path A to B has a length of 1, while A to C is longer with a length of 2.

Step 3 All-Pairs Shortest Path Matrix

To calculate centrality, we must find the most efficient way to travel between every possible pair of nodes in the network. The table lists the Source and Target for every combination. It identifies the Shortest Path based on the weights from Step 2. Total Length: The sum of weights for that path. # Paths: In some cases, there is more than one shortest path with the exact same length (e.g., from B to C, there are two equal paths: B-A-C and B-D-C, both totaling 3).

Step 4 Betweenness Contribution and Final Score

Finally, we calculate the "load" on each specific edge. The Betweenness Centrality of an edge is the sum of the fraction of all-pairs shortest paths that pass through it. Full Credit (1): If an edge is the *only* way to complete a shortest path (like B-D for the trip B to D), it gets 1 full point. Partial Credit (0.5): If there are two equal shortest paths (like for the B to C trip), the edges involved (A-B, A-C, B-D, C-D) each receive only 0.5, reflecting that the "traffic" is split between them. As a Result: Edge B–D has the highest score (2.5), identifying it as the most critical edge in this specific network.

Example 2.

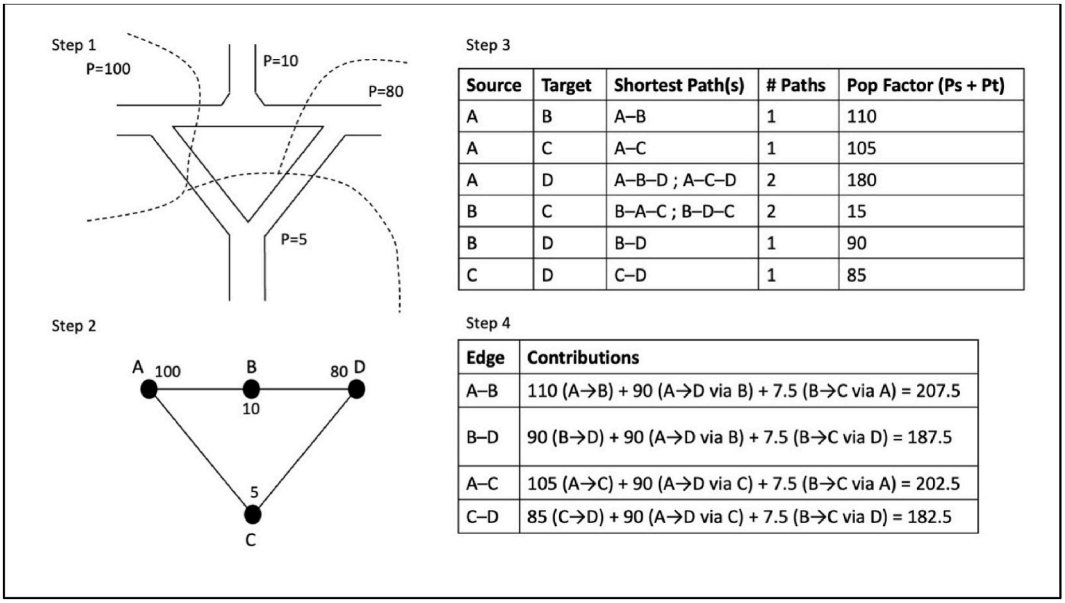

Source	Target	Shortest Path(s)	# Paths	Pop Factor (Ps + Pt)
A	B	A–B	1	110
A	C	A–C	1	105
A	D	A–B–D ; A–C–D	2	180
B	C	B–A–C ; B–D–C	2	15
B	D	B–D	1	90
C	D	C–D	1	85

Edge	Contributions
A–B	110 (A→B) + 90 (A→D via B) + 7.5 (B→C via A) = 207.5
B–D	90 (B→D) + 90 (A→D via B) + 7.5 (B→C via D) = 187.5
A–C	105 (A→C) + 90 (A→D via C) + 7.5 (B→C via A) = 202.5
C–D	85 (C→D) + 90 (A→D via C) + 7.5 (B→C via D) = 182.5

This diagram demonstrates the advanced calculation of Population-based Edge Betweenness Centrality (EBC-Pop). In this model, the "importance" of a road is no longer just about geometry; it is weighted by the number of people who potentially use that road to travel between census areas. Here is the step-by-step description of this process:

Step 1 Spatial Join of Census Data

The real-world map is now overlaid with census area boundaries (dashed lines). Each census area has a specific population value (P). The population is assigned to node according to their vicinity to the nearest census area centroid. For example, the large area with P = 100 is linked to Node A because the closest centroid of the census areas to the node A is the one with P = 100.

Step 2 Population-Weighted Graph

The graph is updated to include population attributes. Nodes (A, B, C, D): Now act as population centers with assigned values: A = 100, B = 10, D = 80, C = 5. Edges: Remain the physical connectors, but their load will now be determined by the population flows between nodes.

Step 3 All-Pairs Flow Matrix (Equation (2))

We calculate the Pop Factor for every pair of nodes. We sum the population of the source and target: Pair A-B: Pop Factor = 100 (A) + 10 (B) = 110}. Pair A-D: Pop Factor = 100 (A) + 80 (D) = 180.

Step 4 PEBC Contribution and Final Criticality

This is the final summation stage where the social importance of each road is revealed. The score for an edge is the sum of (Pop Factor/# Paths) for every trip that crosses it.

Edge A–B: Receives contributions from trips like A to B (110 points), half of the A to D trips (90 points), and half of the B to C trips (7.5 points). Total Score: 207.5. As a result, we now see that Edge A–B has become the most critical infrastructure.

Data availability

Data will be made available on request.

References

[1] UNDRR, Terminology. United Nations Office for Disaster Risk Reduction Geneva, Switzerland, 2020.
[2] S. Mohammadi, S. De Angeli, G. Boni, F. Pirlone, S. Cattari, Review article: current approaches and critical issues in multi-risk recovery planning of urban areas exposed to natural hazards, Nat. Hazards Earth Syst. Sci. 24 (1) (2024) 79–107, https://doi.org/10.5194/nhess-24-79-2024.
[3] Y.-P. Fang, E. Zio, An adaptive robust framework for the optimization of the resilience of interdependent infrastructures under natural hazards, Eur. J. Oper. Res. 276 (3) (Aug. 2019) 1119–1136, https://doi.org/10.1016/j.ejor.2019.01.052.
[4] S. Sobhaninia, S.T. Buckman, Revisiting and adapting the Kates-Pijawka disaster recovery model: a reconfigured emphasis on anticipation, equity, and resilience, Int. J. Disaster Risk Reduct. 69 (Feb. 2022) 102738, https://doi.org/10.1016/j.ijdrr.2021.102738.
[5] L. Savelberg, Y. Casali, M. van den Homberg, J. Zatarain Salazar, T. Comes, Comparing hierarchical and inductive methods reveals fundamental differences in social vulnerability rankings, Sci. Rep. 15 (1) (Oct. 2025) 34541, https://doi.org/10.1038/s41598-025-17860-y.
[6] S. Cara, A. Aprile, L. Pelà, P. Roca, Seismic Risk Assessment and Mitigation at Emergency Limit Condition of Historical Buildings along Strategic Urban Roadways. Application to the 'Antiga Esquerra de L'Eixample' Neighborhood of Barcelona, Int. J. Architect. Herit. 12 (7–8) (Nov. 2018) 1055–1075, https://doi.org/10.1080/15583058.2018.1503376.
[7] C. D'Alpaos, M.R. Valluzzi, Protection of cultural heritage buildings and artistic assets from seismic hazard: a hierarchical approach, Sustainability 12 (4) (Jan. 2020), https://doi.org/10.3390/su12041608. Art. no. 4.
[8] Z. Lin, C. Jia, The optimization model in the disaster risk mitigation investment, Syst. Eng. Procedia 5 (Jan. 2012) 191–197, https://doi.org/10.1016/j.sepro.2012.04.031.
[9] F. Giuliani, A. de Falco, G. Sevieri, and V. Cutini, "Managing emergency into historic centres in Italy: seismic vulnerability evaluation at urban scale," COMPDYN Proceedings. Accessed: August. 15, 2022. [Online]. Available: https://2019.compdyn.org/.
[10] K. Skrame, et al., Earthquake-Resistant Cities in Albania: the Seismic Microzonation Studies (SMS) and Limit Condition in Emergency (LCE) Integrated Approach, 2020, p. 7.
[11] V. Tomassoni, M.S. Benigni, C. Fontana, M. Giuffrè, Tra settorialità e necessità di integrazione: la CLE nelle politiche di mitigazione del rischio sismico, Territorio (2024) 2023/106, https://doi.org/10.3280/TR2023-106015.
[12] D. Alexander, An evaluation of the recovery strategy after 6 April 2009 earthquake in L'Aquila, central Italy. Disaster Planning and Emergency Management, 2010.
[13] M. Clemente, L. Salvati, Interrupted' landscapes: Post-Earthquake reconstruction in between urban renewal and social identity of local communities, Sustainability 9 (11) (Nov. 2017), https://doi.org/10.3390/su9112015. Art. no. 11.
[14] D. Contreras, T. Blaschke, M.E. Hodgson, Lack of spatial resilience in a recovery process: case L'Aquila, Italy, Technol. Forecast. Soc. Change 121 (Aug. 2017) 76–88, https://doi.org/10.1016/j.techfore.2016.12.010.
[15] S. Mohammadi, et al., Fuzzy cognitive mapping to uncover vital urban functions and their interdependencies for disaster recovery, J. Contingencies Crisis Manag. 33 (3) (2025) e70071, https://doi.org/10.1111/1468-5973.70071.
[16] S. Cattari, D. Ottonelli, S. Mohammadi, EQ-DIRECTION procedure towards an improved urban seismic resilience: application to the pilot case Study of sanremo municipality, Sustainability 16 (6) (Jan. 2024), https://doi.org/10.3390/su16062501. Art. no. 6.
[17] C. Curt, Multirisk: what trends in recent works? – a bibliometric analysis, Sci. Total Environ. 763 (Apr. 2021) 142951, https://doi.org/10.1016/j.scitotenv.2020.142951.
[18] S. Hochrainer-Stigler, et al., Toward a framework for systemic multi-hazard and multi-risk assessment and management, iScience 26 (5) (May 2023) 106736, https://doi.org/10.1016/j.isci.2023.106736.
[19] P.J. Ward, et al., Invited perspectives: a research agenda towards disaster risk management pathways in multi-(hazard-)risk assessment, Nat. Hazards Earth Syst. Sci. 22 (4) (Apr. 2022) 1487–1497, https://doi.org/10.5194/nhess-22-1487-2022.
[20] T. Görüm, et al., The 2023 Türkiye-Syria earthquake disaster was exacerbated by an atmospheric river, Commun. Earth Environ. 6 (1) (Feb. 2025) 1–10, https://doi.org/10.1038/s43247-025-02111-9.
[21] N.Y. Aydin, K. Celik, R. Gecen, S. Kalaycioglu, S. Duzgun, Rebuilding Antakya: cultivating urban resilience through cultural identity and education for post-disaster reconstruction in Turkey, Int. J. Disaster Risk Reduct. 117 (Feb. 2025) 105196, https://doi.org/10.1016/j.ijdrr.2025.105196.
[22] N.Y. Aydin, S. Balakrishnan, M. van der Jagt, "Systemic Resilience under Compound Hazards: insights into Multi-Hazard Earthquake–Flood Recovery Dynamics in Antakya,", Copernicus Meetings (Mar) (2026) https://doi.org/10.5194/egusphere-egu26-10941. EGU26-10941.
[23] R. Der Sarkissian, C. Abdallah, J.-M. Zaninetti, S. Najem, Modelling intra-dependencies to assess road network resilience to natural hazards, Nat. Hazards 103 (1) (Aug. 2020) 121–137, https://doi.org/10.1007/s11069-020-03962-5.
[24] R. Gentile, C. Galasso, Y. Idris, I. Rusydy, E. Meilianda, From rapid visual survey to multi-hazard risk prioritisation and numerical fragility of school buildings, Nat. Hazards Earth Syst. Sci. 19 (7) (Jul. 2019) 1365–1386, https://doi.org/10.5194/nhess-19-1365-2019.
[25] M.C. de Ruiter, A.F. Van Loon, The challenges of dynamic vulnerability and how to assess it, iScience 25 (8) (2022).
[26] M.C. de Ruiter, A. Couasnon, M.J. van den Homberg, J.E. Daniell, J.C. Gill, P.J. Ward, Why we can no longer ignore consecutive disasters, Earths Future 8 (3) (2020) e2019EF001425.
[27] M.C. de Ruiter, J.A. de Bruijn, J. Englhardt, J.E. Daniell, H. de Moel, P.J. Ward, The asynergies of structural disaster risk reduction measures: comparing floods and earthquakes, Earths Future 9 (1) (2021), https://doi.org/10.1029/2020EF001531 e2020EF001531.
[28] K. Otárola, L. Iannacone, R. Gentile, C. Galasso, Multi-hazard life-cycle consequence analysis of deteriorating engineering systems, Struct. Saf. 111 (Nov. 2024) 102515, https://doi.org/10.1016/j.strusafe.2024.102515.
[29] D.T. Cook, A.B. Liel, A. Safiey, Earthquake functional recovery in modern reinforced concrete buildings, J. Struct. Eng. 150 (9) (Sep. 2024) 04024117, https://doi.org/10.1061/JSENDH.STENG-12904.
[30] C. Molina Hutt, T. Vahanvaty, P. Kourehpaz, An analytical framework to assess earthquake-induced downtime and model recovery of buildings, Earthq. Spectra 38 (2) (May 2022) 1283–1320, https://doi.org/10.1177/87552930211060856.
[31] F. Guzzetti, et al., Landslides triggered by the 23 November 2000 rainfall event in the Imperia Province, Western Liguria, Italy, Eng. Geol. 73 (3) (Jun. 2004) 229–245, https://doi.org/10.1016/j.enggeo.2004.01.006.
[32] EUROPEAN COMMISSION, EU Preparedness Union Strategy to prevent and react to emerging threats and crises [Online]. Available: https://ec.europa.eu/commission/presscorner/detail/en/ip_25_856, 2025. (Accessed 30 March 2025).
[33] Mappe - Geoportal Regione Liguria." Accessed: May 23, 2026. [Online]. Available: https://geoportal.regione.liguria.it/catalogo/mappe.html.
[34] M. Stucchi, C. Meletti, V. Montaldo, H. Crowley, G.M. Calvi, E. Boschi, Seismic hazard assessment (2003–2009) for the Italian building code, Bull. Seismol. Soc. Am. (Aug. 2011), https://doi.org/10.1785/0120100130.
[35] C. Meletti, V. Montaldo, M. Stucchi, F. Martinelli, Database Della Pericolosità Sismica MPS04, Istituto Nazionale di Geofisica e Vulcanologia (INGV), 2006 [Online]. Available: http://esse1.mi.ingv.it/. (Accessed 18 April 2026).
[36] G. Forte, E. Chioccarelli, M. De Falco, P. Cito, A. Santo, I. Iervolino, Seismic soil classification of Italy based on surface geology and shear-wave velocity measurements, Soil Dynam. Earthq. Eng. 122 (Jul. 2019) 79–93, https://doi.org/10.1016/j.soildyn.2019.04.002.
[37] L.C. Freeman, Centrality in social networks conceptual clarification, Soc. Netw. 1 (3) (Jan. 1978) 215–239, https://doi.org/10.1016/0378-8733(78)90021-7.
[38] L.C. Freeman, A set of measures of centrality based on betweenness, Sociometry 40 (1) (1977) 35–41, https://doi.org/10.2307/3033543.
[39] M. Barthelemy, Time evolution of road networks, in: M. Chraibi, M. Boltes, A. Schadschneider, A. Seyfried (Eds.), Traffic and Granular Flow '13, Springer International Publishing, Cham, 2015, pp. 317–337, https://doi.org/10.1007/978-3-319-10629-8_38.
[40] E. Strano, V. Nicosia, V. Latora, S. Porta, M. Barthélemy, Elementary processes governing the evolution of road networks, Sci. Rep. 2 (1) (Mar. 2012) 296, https://doi.org/10.1038/srep00296.

[41] Y. Casali, N.Y. Aydin, T. Comes, A data-driven approach to analyse the co-evolution of urban systems through a resilience lens: a Helsinki case study, Environ. Plan. B Urban Anal. City Sci. (Feb. 2024), https://doi.org/10.1177/23998083241235246.
[42] N.Y. Aydin, H.S. Duzgun, F. Wenzel, H.R. Heinimann, Integration of stress testing with graph theory to assess the resilience of urban road networks under seismic hazards, Nat. Hazards 91 (1) (Mar. 2018) 37–68, https://doi.org/10.1007/s11069-017-3112-z.
[43] W.A. Marra, M.G. Kleinhans, E.A. Addink, Network concepts to describe channel importance and change in multichannel systems: test results for the Jamuna River, Bangladesh, Earth Surf. Process. Landf. 39 (6) (2014) 766–778, https://doi.org/10.1002/esp.3482.
[44] N.Y. Aydin, Y. Casali, H. Sebnem Duzgun, H.R. Heinimann, Identifying changes in critical locations for transportation networks using centrality, in: S. Geertman, Q. Zhan, A. Allan, C. Pettit (Eds.), Computational Urban Planning and Management for Smart Cities, Springer International Publishing, Cham, 2019, pp. 405–423, https://doi.org/10.1007/978-3-030-19424-6_22.
[45] S. Porta, et al., Street centrality and the location of economic activities in Barcelona, Urban Stud. 49 (7) (May 2012) 1471–1488, https://doi.org/10.1177/0042098011422570.
[46] S. Porta, P. Crucitti, V. Latora, The network analysis of urban streets: a primal approach, Environ. Plann. Plann. Des. 33 (5) (Oct. 2006) 705–725, https://doi.org/10.1068/b32045.
[47] F.J. Goerlich Gisbert, I. Cantarino Martí, E. Gielen, Clustering cities through urban metrics analysis, J. Urban Des. 22 (5) (Sep. 2017) 689–708, https://doi.org/10.1080/13574809.2017.1305882.
[48] B. Şenik, O. Uzun, An assessment on size and site selection of emergency assembly points and temporary shelter areas in Düzce, Nat. Hazards 105 (2) (Jan. 2021) 1587–1602, https://doi.org/10.1007/s11069-020-04367-0.
[49] S. Lagomarsino, S. Cattari, D. Ottonelli, The heuristic vulnerability model: fragility curves for masonry buildings, Bull. Earthq. Eng. 19 (8) (Jun. 2021) 3129–3163, https://doi.org/10.1007/s10518-021-01063-7.
[50] S. Lagomarsino, S. Giovinazzi, Macroseismic and mechanical models for the vulnerability and damage assessment of current buildings, Bull. Earthq. Eng. 4 (4) (Nov. 2006) 415–443, https://doi.org/10.1007/s10518-006-9024-z.
[51] S. Ghimire, P. Guéguen, A. Astorga, Analysis of the efficiency of intensity measures from real earthquake data recorded in buildings, Soil Dynam. Earthq. Eng. 147 (Aug. 2021) 106751, https://doi.org/10.1016/j.soildyn.2021.106751.
[52] N. Luco, C.A. Cornell, Structure-Specific scalar intensity measures for near-source and ordinary earthquake ground motions, Earthq. Spectra 23 (2) (May 2007) 357–392, https://doi.org/10.1193/1.2723158.
[53] A.K. Kazantzi, D. Vamvatsikos, Intensity measure selection for vulnerability studies of building classes, Earthq. Eng. Struct. Dynam. 44 (15) (2015) 2677–2694, https://doi.org/10.1002/eqe.2603.
[54] M. Dolce, et al., Seismic risk assessment of residential buildings in Italy, Bull. Earthq. Eng. 19 (8) (Jun. 2021) 2999–3032, https://doi.org/10.1007/s10518-020-01009-5.
[55] M.G.B. Merani, D. Sivori, S. Lagomarsino, S. Barani, S. Cattari, Sensitivity of urban seismic damage predictions to input data detail: an application to Sanremo, Italy, Bull. Earthq. Eng. 24 (4) (Apr. 2026) 2317–2347, https://doi.org/10.1007/s10518-026-02371-6.
[56] G. Zuccaro, F. Cacace, Seismic casualty evaluation: the Italian model, an application to the L'Aquila 2009 event, in: R. Spence, E. So, C. Scawthorn (Eds.), Human Casualties in Earthquakes: Progress in Modelling and Mitigation, Springer Netherlands, Dordrecht, 2011, pp. 171–184, https://doi.org/10.1007/978-90-481-9455-1_12.
[57] M. Mehaffy, S. Porta, Y. Rofè, N. Salingaros, Urban nuclei and the geometry of streets: the 'emergent neighborhoods' model, Urban Des. Int. 15 (1) (Mar. 2010) 22–46, https://doi.org/10.1057/udi.2009.26.
[58] A. Walmsley, Greenways and the making of urban form, Landsc. Urban Plann. 33 (1) (Oct. 1995) 81–127, https://doi.org/10.1016/0169-2046(95)02015-L.
[59] N.C. Dinh, F. Ubukata, N.Q. Tan, V.H. Ha, How do social connections accelerate post-flood recovery? Insights from a survey of rural households in central Vietnam, Int. J. Disaster Risk Reduct. 61 (Jul. 2021) 102342, https://doi.org/10.1016/j.ijdrr.2021.102342.
[60] S. Platt, O. Carpenter, F. Mahdavian, A. Coburn, Disaster recovery – evidence from 100 natural disasters, Int. J. Disaster Risk Reduct. (Aug. 2025) 105764, https://doi.org/10.1016/j.ijdrr.2025.105764.
[61] S. De Angeli, B.D. Malamud, L. Rossi, F.E. Taylor, E. Trasforini, R. Rudari, A multi-hazard framework for spatial-temporal impact analysis, Int. J. Disaster Risk Reduct. 73 (2022) 102829, https://doi.org/10.1016/j.ijdrr.2022.102829.
[62] R. Nelson, M. Warnier, T. Verma, Conceptualizing urban inequalities as a complex socio-technical phenomenon, Geogr. Anal. 56 (2) (2024) 187–216, https://doi.org/10.1111/gean.12373.
[63] L. Nicoletti, M. Sirenko, T. Verma, Disadvantaged communities have lower access to urban infrastructure, Environ. Plan. B Urban Anal. City Sci. 50 (3) (Mar. 2023) 831–849, https://doi.org/10.1177/23998083221131044.
[64] F. Huang, J. Tang, P. Zhao, Z. Chen, J. Li, W. Lyu, Human mobility under disasters: a systematic review and framework for equitable and resilient mobility governance, npj Nat. Hazards 2 (1) (Nov. 2025) 99, https://doi.org/10.1038/s44304-025-00153-9.
[65] G. E. Machlis, M. O. Román, and S. T. A. Pickett, "A framework for research on recurrent acute disasters," Sci. Adv., vol. 8, no. 10, p. eabk2458, doi: 10.1126/sciadv.abk2458.
[66] V. Spagnoli, C. Piferi, Regeneration of Historic Centers in Mediterranean Cities: the Case Study of the Venice District in Livorno, Firenze University Press, 2023 [Online]. Available: https://flore.unifi.it/handle/2158/1302082. (Accessed 10 December 2025).
[67] M.S. Dastjerdi, A. Lak, Towards resilient place emphasizing urban form: an assessment framework in urban design, Sustain. Cities Soc. 96 (Sep. 2023) 104646, https://doi.org/10.1016/j.scs.2023.104646.
[68] S. Meerow, J.P. Newell, M. Stults, Defining urban resilience: a review, Landsc. Urban Plann. 147 (Mar. 2016) 38–49, https://doi.org/10.1016/j.landurbplan.2015.11.011.
[69] G. Datola, Implementing urban resilience in urban planning: a comprehensive framework for urban resilience evaluation, Sustain. Cities Soc. 98 (Nov. 2023) 104821, https://doi.org/10.1016/j.scs.2023.104821.
[70] S. Ashja-Ardalan, A.A. Alesheikh, M. Sharif, D. Wittowsky, Resilience of urban road networks to climate change: a spatial-topological approach, Transport. Res. Transport Environ. 148 (Nov. 2025) 104948, https://doi.org/10.1016/j.trd.2025.104948.
[71] G. Boeing, J. Ha, Resilient by design: simulating street network disruptions across every urban area in the world, Transport. Res. Pol. Pract. 182 (Apr. 2024) 104016, https://doi.org/10.1016/j.tra.2024.104016.
[72] X. Wang, et al., A new flow-based centrality method for identifying statistically significant centers, Sustain. Cities Soc. 99 (Dec. 2023) 104984, https://doi.org/10.1016/j.scs.2023.104984.
[73] S. Krishnan, N.Y. Aydin, T. Comes, TIMEWISE: Temporal Dynamics for Urban Resilience - theoretical insights and empirical reflections from Amsterdam and Mumbai, npj Urban Sustain 4 (1) (Jan. 2024) 4, https://doi.org/10.1038/s42949-024-00140-5.
[74] A. FathiAzar, S. De Angeli, S. Cattari, Towards integrated multi-risk reduction strategies: a catalog of flood and earthquake risk mitigation measures at the building and neighborhood scales, Int. J. Disaster Risk Reduct. 113 (Oct. 2024) 104884, https://doi.org/10.1016/j.ijdrr.2024.104884.